This research has been co-financed by the European Union (European Social Fund, ESF) and Greek national funds through the Operational Program "Education and Lifelong Learning" of the National Strategic Reference Framework (NSRF), under the grants schemes "Funding of proposals that have received a positive evaluation in the 3rd and 4th Call of ERC Grant Schemes" and the program "Thales"

European Union
European Social Fund

OPERATIONAL PROGRAMME
EDUCATION AND LIFELONG LEARNING
investing in knowledge society
MINISTRY OF EDUCATION & RELIGIOUS AFFAIRS, CULTURE & SPORTS
MANAGING AUTHORITY

NSRF
2007-2013
programme for development
EUROPEAN SOCIAL FUND

Co-financed by Greece and the European Union

CERN Theory Seminar, 27 November 2013

Holographic models for QCD in the Veneziano limit

Elias Kiritsis

CERN University of Crete APC, Paris

Introduction

• YM theory is the basis for the definition of QCD. It has a deceptively simple Lagrangian that hides the complexity of dynamics.

• Many approaches have been developed to master its dynamics. We do understand well today its equilibrium/euclidean dynamics, even at strong coupling. We understand much less the non-equilibrium dynamics and multi-body processes at strong coupling.

• Quarks provide an extra layer of complexity despite their simple action. They are responsible for a large part of the phenomenology of real world QCD.

• The most important new ingredient in the presence of quarks is flavor (chiral) symmetry and its dynamical breaking.

• Apart for their presence as sources in the theory, the quark quantum effects may be important. The importance may vary depending on observables.

• Sometimes the relevant physics can be studied in the "Quenched Approximation": quarks have a small backreaction on the glue dynamics. Several interesting phenomena have been studied in this context.

• I will use the following "definition" : QCD = an SU(N_c) gauge theory with N_f fundamental quarks.

• For several other phenomena, it is important to include propagating quarks and their quantum corrections in order to study them. In this second class we can mention:

♠ **The conformal window:** the theory is expected flows to an IR CFT for $x \equiv \frac{N_f}{N_c} \geq x_c$ if quarks are massless. The chiral symmetry is expected to remain unbroken in this phase. The conformal window ends above at the Banks-Zaks point, $x = \frac{11}{2}$.

Banks+Zaks

♠ The **phase transition** at $x = x_c$ that is conjectured to be in the BKT class. This type of transition where for $x < x_c$ there is a non-zero chiral condensate is known as a conformal transition.

Miransky, Kaplan+Stephanov+Son

♠ The region just below x_c where the theory is expected to exhibit walking behavior. This type of behavior has been advocated to be crucially useful for technicolor models.

♠ The QCD thermodynamics as a function of x.

♠ The phase diagram as a function of baryon density. Here we expect a color superconducting phase, as well as a color-flavor locking phase.

Alford+Rajagopal+Wilczek

• All of the phenomena above except those in the Banks-Zaks region are at strong coupling and therefore difficult to analyze.

• Several (controlable and uncontrolable) techniques were applied so far for their study.

• Lattice calculations have practical problems with the fate of chiral symmetry and massless (light) quarks. The reasons are a combination of lattice doubling, finite volume effects and finite computing capacity. Despite progress, the presence of the conformal window in lattice calculations is still speculative.

DelDebbio lattice review 2011

• Truncated Schwinger-Dyson equations, gap equations, guesswork on β functions, effective theories etc. It is with such techniques that some of the expectations above were found. There is no consensus, however on many of the phenomena.

• The purpose of our effort is to explore the construction of holographic models that describe similar dynamics, so that:

(a) Explore the landscape of possibilities

(b) Construct realistic strong coupling models of QCD

The 't Hooft Large N_c limit

• The large N_c limit offers a non-perturbative tool into strong coupling physics.

• The 't Hooft large N_c limit is defined as

$$N_c \to \infty, \qquad \lambda = g^2_{\text{YM}} N_c \to \text{fixed} \quad , \quad N_f \quad \text{fixed}$$

• As N_f is kept fixed while $N_c \to \infty$, $N_f \ll N_c$ and it always samples the "quenched" approximation.

• The planar (sphere) diagrams give the dominant contribution, $O(N_c^2)$.

• Fermion loops (boundaries of the Riemann surface) give subleading contributions in $1/N_c$ (each loop costs a factor of $\frac{N_f}{N_c}$).

• Because $x \equiv \frac{N_f}{N_c} \to 0$ in the 't Hooft limit, we cannot capture any of the effects for which the presence of flavor is important.

The Veneziano limit

• The proper limit in order to study the previous phenomena in the large N_c approximation is the limit introduced by Veneziano in (1976)

$$N_c \to \infty \quad , \quad N_f \to \infty \quad , \quad \frac{N_f}{N_c} = x \to \text{fixed} \quad , \quad \lambda = g^2_{\mathrm{YM}} N_c \to \text{fixed}$$

• In terms of the dual string theory, the boundaries of diagrams are not suppressed anymore: $\frac{N_f}{N_c} \sim \mathcal{O}(1)$ and surfaces with an arbitrary number of boundaries contribute at the same order in $1/N_c$.

• QCD in the Veneziano limit is solvable in 2d, but in 4d it provides a formidable problem, (seemingly) much harder than the 't Hooft limit.

The Veneziano limit in string theory

• Implementing the Veneziano limit in string theory is so far a very difficult problem, with very little progress achieved.

• The main reason is that the backreaction of probe branes (carrying the flavor degrees of freedom) is very difficult to handle.

• Techniques where the flavor branes were "smeared" in transverse space have provided some string models for addressing the Veneziano limit.

Kiritsis+Kounnas+Petropoulos+Rizos, '02, Bigazzi+Casero+Cotrone+Kiritsis+Paredes, '05

Casero+Nunez+Paredes, '06

• No major progress in the controlled construction of the string theory configurations has been achieved so far.

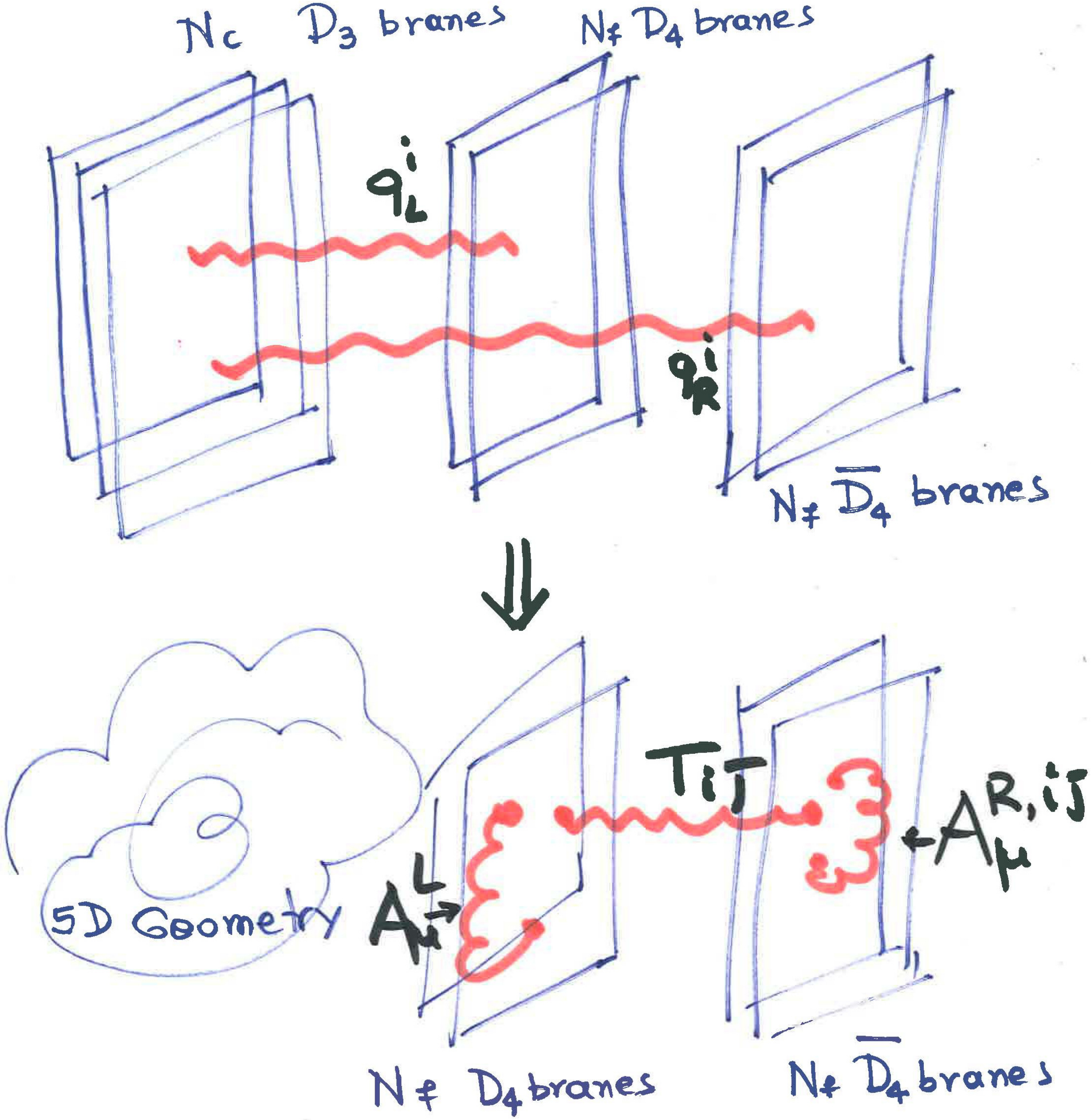

Nc D3 branes
Nf D4 branes
q^i_L
q^i_R
Nf $\bar{D}_4$ branes
5D Geometry
A^L_μ
T_{ij}
$A^{R,ij}_\mu$
Nf D4 branes
Nf $\bar{D}_4$ branes

The Banks-Zaks region

- The QCD β function in the Veneziano limit is

$$\dot{\lambda} = \beta(\lambda) = -b_0\lambda^2 + b_1\lambda^3 + \mathcal{O}(\lambda^4) \ , \ \ b_0 = \frac{2}{3}\frac{(11-2x)}{(4\pi)^2} \ , \ \ b_1 = -\frac{2}{3}\frac{(34-13x)}{(4\pi)^4}$$

- For $x > \frac{11}{2}$ the theory is IR free.

- Notice that at $x = \frac{11}{2}$, $b_0 = 0$, $b_1 > 0$.

- The Banks-Zaks region is

$$x = \frac{11}{2} - \epsilon \quad \text{with} \quad 0 < \epsilon \ll 1$$

- We obtain a fixed point of the β-function at

$$\lambda_* \simeq \frac{(8\pi)^2}{75}\epsilon + \mathcal{O}(\epsilon^2)$$

which is trustable in perturbation theory, as λ_* can be made arbitrarily small.

• The mass operator, $\bar{\psi}_L\psi_R$ has now dimension smaller than three, from the perturbative anomalous dimension (in the V-limit)

$$-\frac{d\log m}{d\log\mu}\equiv\gamma=\frac{3}{(4\pi)^2}\lambda+\frac{(203-10x)}{12\,(4\pi)^4}\lambda^2+\mathcal{O}(\lambda^3,N_c^{-2})$$

• Extrapolating to lower x we expect the phase diagram

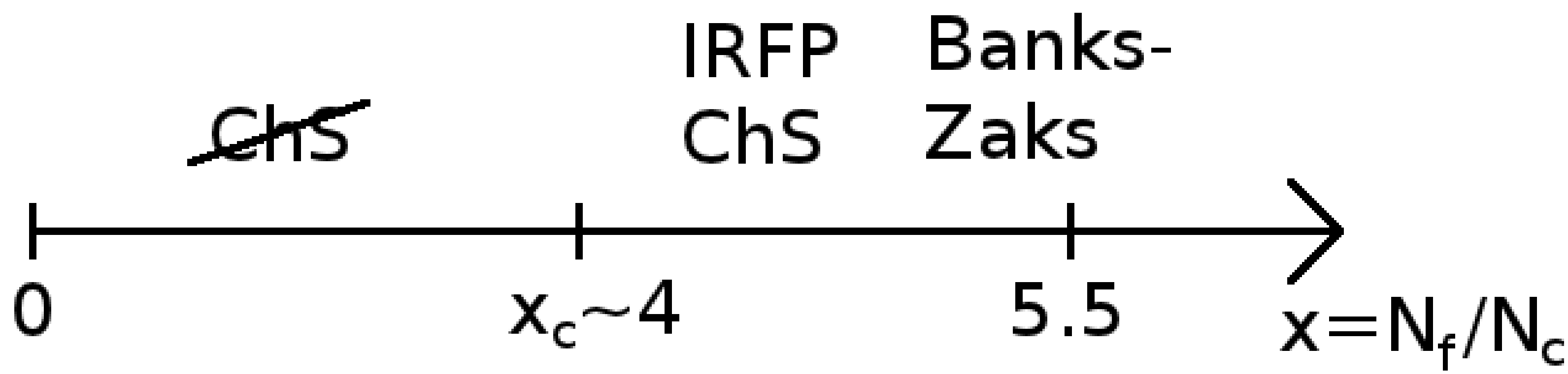

Walking region+Technicolor (TC)

• Technicolor: EW symmetry breaking is due to a new strong gauge interaction with $\Lambda_{TC} \sim 1TeV$.

• The EW Higgs is scalar TC meson and the vev is due to a condensate of TC fermions $\langle H \rangle \sim \langle \bar{\psi}_{TC} \psi_{TC} \rangle$ from TC chiral symmetry breaking.

• The Higgs vev is the TechniColor f_π and should be set to $\sim$ 250 GeV.

• The composite Higgs couplings to the SM fermions χ are now four-fermi terms,

$$H \bar{\chi} \chi \sim \bar{\psi}_{TC} \psi_{TC} \; \bar{\chi} \chi$$

and should be generated by a new (ETC) interaction at a higher scale, Λ_{ETC}.

• There are some important problems with this idea:

♠ At the qualitative level: it relies on non-perturbative physics and therefore is not easily controlable/calculable.

♠ There can be important flavor changing processes (that are suppressed in the SM)

♠ To get the correct size for all masses, the dimension of operators $\psi_{TC}\psi_{TC}$ must be close to two (instead of 3 in perturbation theory).

♠ The dimensionless quantity S controls the low-energy corrections to EW gauge boson kinetic terms

Peskin+Takeuchi

$$S = \frac{d}{dq^2}(\Pi_V(q^2) - \Pi_A(q^2))\Big|_{q^2=0} \quad , \quad \left(\delta_{\mu\nu} - \frac{q_\mu q_\nu}{q^2}\right)\Pi_i(q^2) \equiv \langle J^i_\mu(q) J^i_\nu(0)\rangle$$

is $\mathcal{O}(1)$ in generic theories from the spectral decomposition+sum rules, but EW data imply that additional contributions should be $\mathcal{O}(10^{-2})$.

♠ It has been argued by many scientists that a way out of the above is a TC theory that is near conformal ("walking") and strongly coupled in the TC regime,

Holdom, Appelquist+Karabali+Wijewardhana

♠ Because $S = 0$ in the conformal window it was argued by continuity that $S \to 0$ in the walking region.

Appelquist+Sannino

♠ Because of approximate scale invariance, the theory was expected to have a light scalar, "the dilaton", namely the singlet scalar meson (σ-meson).

Yamawaki+Bando+Matumoto

♠ Despite a lot of work in the last 15 years, whether such a theory exists, and whether it has the required properties has remained elusive till now, especially because lattice techniques are hard to apply to almost massless setups.

The strategy

• Construct (toy) holographic models resembling QCD in the Veneziano limit.

• Put together two ingredients: the holographic model for glue developed earlier: IHQCD

Gursoy+E.K+Nitti

• and the model for flavor based in Sen's tachyon action in string theory (brane-antibrane pairs).

Casero+E.K.+Paredes, Iatrakis+E.K.+Paredes

Immediate Drawbacks:

a) No controlled stringy construction of the background.

b) Quantum effects from light states are unsuppressed.

The holographic models: glue

For YM, ihQCD is a well-tested holographic, string-inspired bottom-up model with action

Gursoy+Kiritsis+Nitti, Gubser+Nelore

$$\mathcal{S}_{\rm g} = M^3 N_c^2 \int d^5x \sqrt{g} \left[R - \frac{4}{3}(\partial\phi)^2 + V_g(\phi) \right]$$

and "vacuum" described by a Poincaré-invariant metric and running dilaton (gauge coupling)

$$ds^2 = e^{2A(r)}(dr^2 + \eta_{\mu\nu}dx^\mu dx^\nu)$$

- The potential V_g $\leftrightarrow$ QCD β-function
- the "scale factor" A $\leftrightarrow$ $\log\mu$ energy scale.
- e^ϕ $\leftrightarrow$ λ 't Hooft coupling

In the UV $\lambda \to 0$ and

$$V_g = V_0 + V_1\lambda + V_2\lambda^2 + \mathcal{O}(\lambda^3)$$

In the IR $\lambda \to \infty$ and

$$V_g \sim \lambda^{\frac{4}{3}}\sqrt{\log\lambda} + \cdots$$

• With an appropriate tuning of two parameters in V_g the model describes well both $T = 0$ glueball spectra as well as thermodynamics.

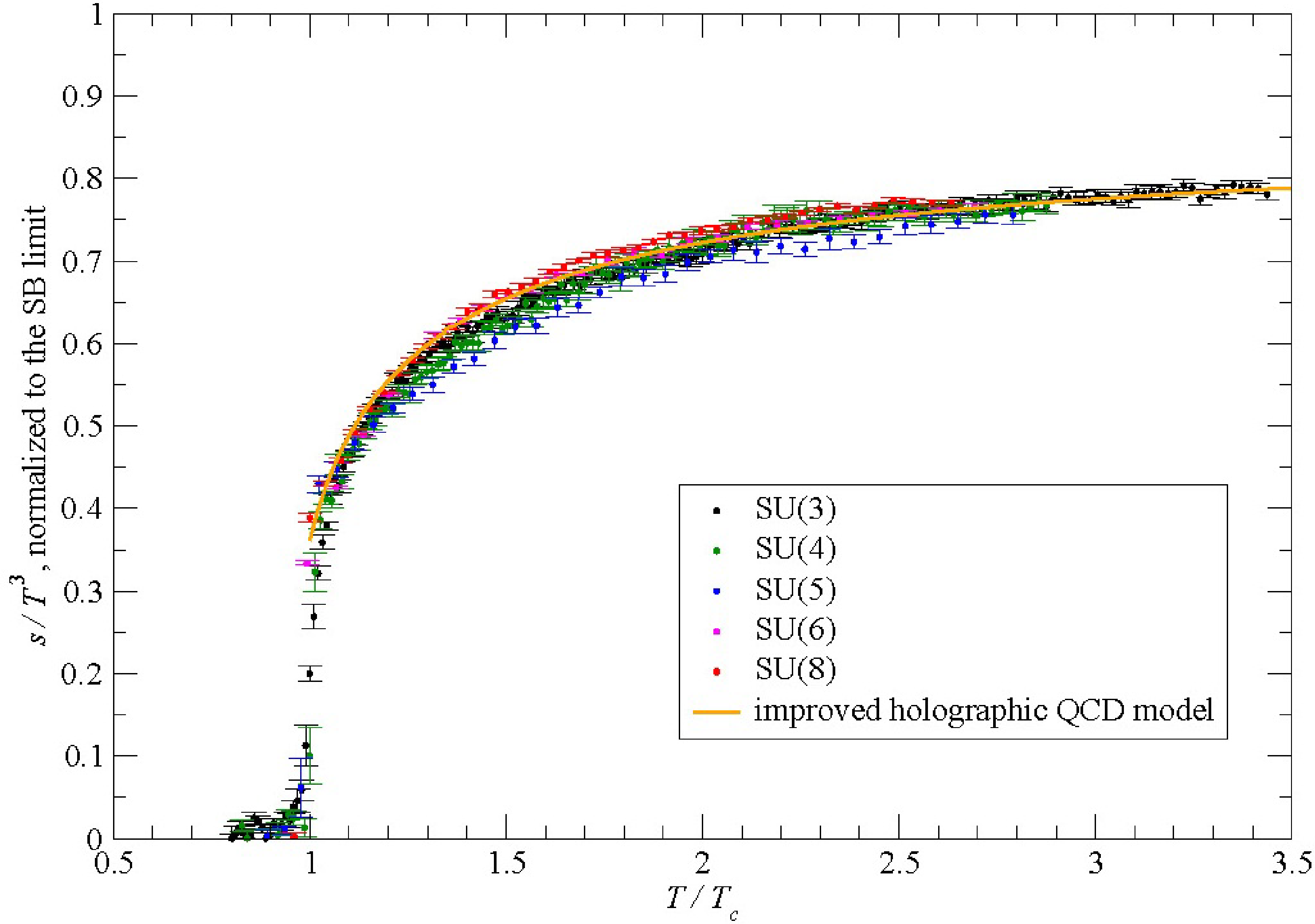

Figure 4: (Color online) Same as in fig. 1, but for the s/T^3 ratio, normalized to the SB limit.

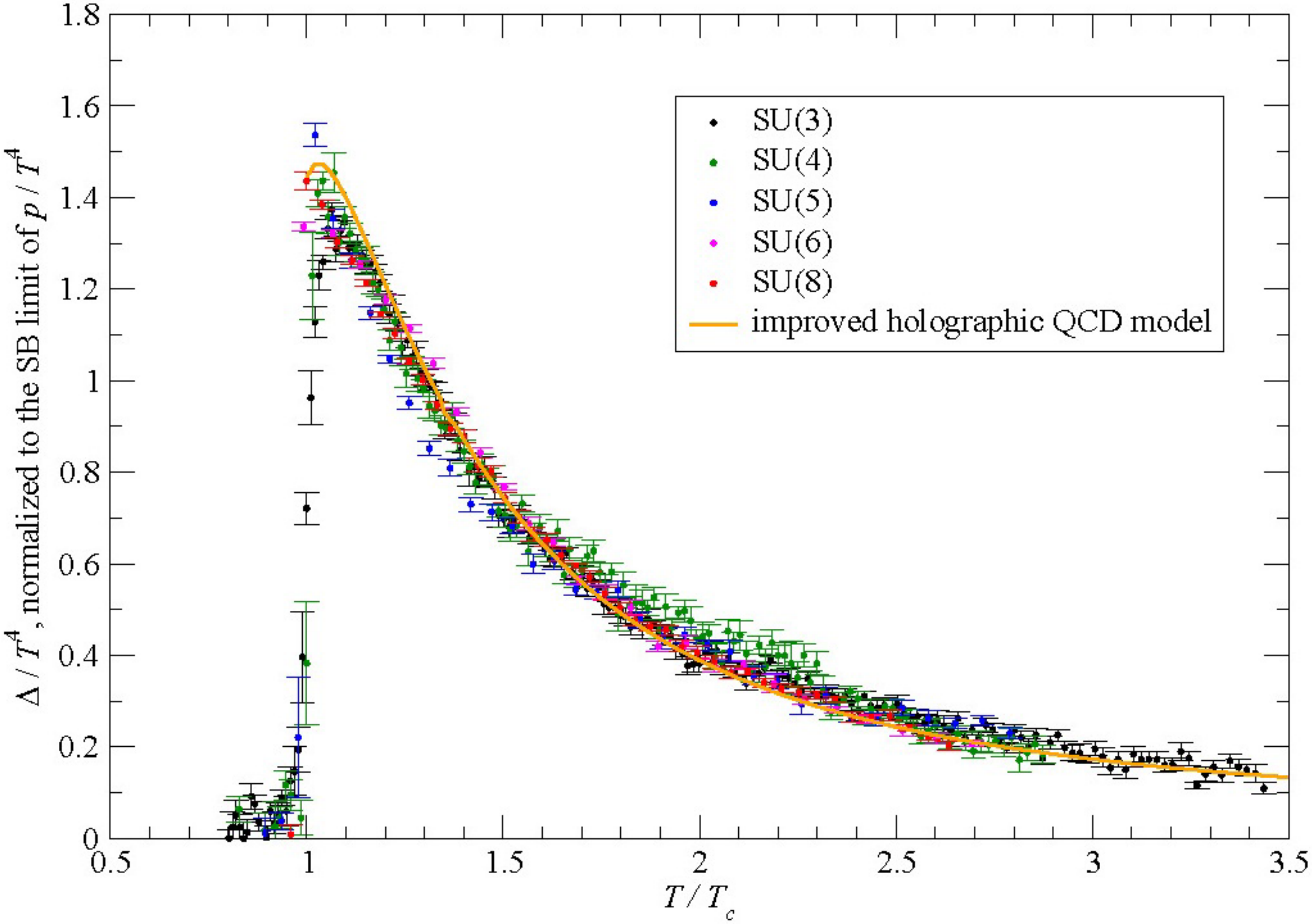

Figure 2: (Color online) Same as in fig. 1, but for the Δ/T^4 ratio, normalized to the SB limit of p/T^4.

Panero

The holographic models: flavor

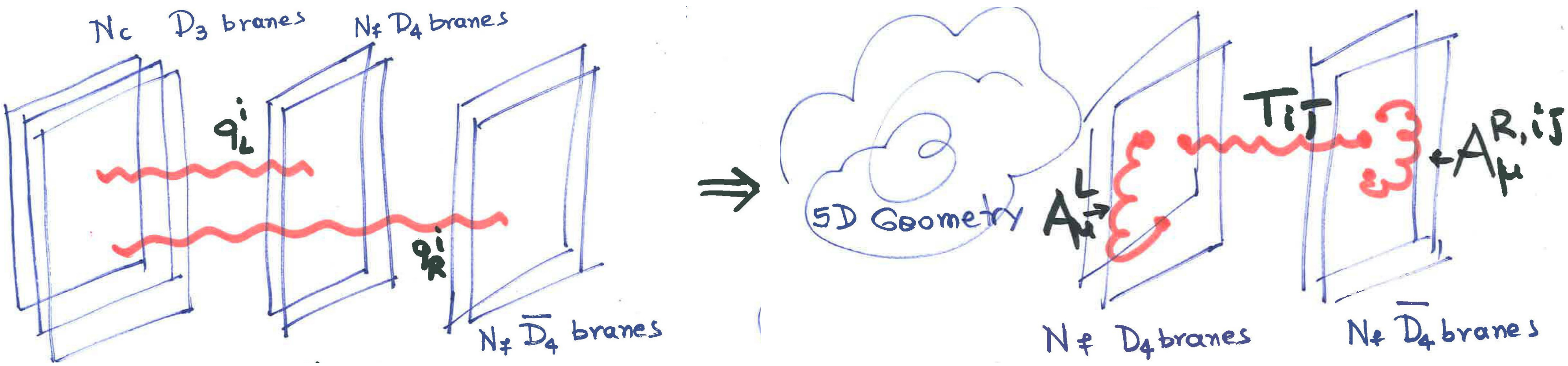

• There are three important operators in the flavor sector,

$$J_\mu^{L,R} = \bar{q}^{L,R}\ \gamma_\mu\ q^{L,R} \quad , \quad \bar{q}_L q_R$$

and their dual fields: $A_\mu^{L,R}$, T that realize the global $U(N_f)_L \times U(N_f)_R$ symmetry.

• An action for the tachyon was given by Sen and has been advocated as the proper dynamics of the chiral, condensate giving in general all the expected features of χSB.

Casero+Kiritsis+Paredes

$$\mathcal{S}_{\text{TDBI}} = -N_f N_c M^3 \int d^5x\ V_f(T)\ e^{-\phi} \sqrt{-\det(g_{ab} + \partial_a T \partial_b T + F_{ab})}$$

$$V(T) = V_0 e^{-aT^2}$$

Kutasov+Marino+Moore

Fusion

The idea is to put together the two ingredients in order to study the chiral dynamics and its backreaction to glue.

$$\mathcal{S} = N_c^2\ M^3 \int d^5x\sqrt{g}\left[R - \frac{4}{3}\frac{(\partial\lambda)^2}{\lambda^2} + V_g(\lambda)\right] -$$

$$-N_f N_c\ M^3 \int d^5x V_f(\lambda, T)\sqrt{-\det(g_{ab} + h(\lambda)\partial_a T \partial_b T)}$$

with the "adiabatic ansatz"

$$V_f(\lambda, T) = V_0(\lambda)\ \exp(-a(\lambda)T^2)$$

Kutasov+Marino+Moore

- We must choose $V_0(\lambda), a(\lambda), h(\lambda)$. How to determine them?

- In the UV ($\lambda \to 0$), they can be adapted to the QCD β function and mass anomalous dimension (two loops).

• In the IR, we need to scan all possibilities: We impose

(a) Existence of a fixed point in the potential in the theory without chiral symmetry breaking.

(b) Asymptotically linear trajectories for mesons.

• The surprise: $V_0(\lambda), a(\lambda), h(\lambda)$ have as $\lambda \to \infty$ the values they have in naive flat space string theory corrected by logs.

$$V_0(\lambda) \sim \lambda^{\frac{7}{3}} \quad , \quad a(\lambda) \sim \lambda^0 \quad , \quad h(\lambda) \sim \lambda^{-\frac{4}{3}} \quad , \quad V_g(\lambda) \sim \lambda^{\frac{4}{3}}$$

• Most of the qualitative physics depends very little on the intermediate regime in λ.

• For every x there are two extrema of the potentials:

♠ $T_* = 0$, we have an IR fixed point at $\lambda = \lambda_*(x_f)$.

♠ $T_* = \infty$, $V_{eff} = V_g(\lambda)$ with no fixed points.

Parameters

• A theory with a single relevant (or marginally relevant) coupling like YM has no parameters.

• The same applies to QCD with massless quarks.

• QCD with all quarks having mass m has a single (dimensionless) parameter : $\frac{m}{\Lambda_{QCD}}$.

• After various rescalings this single parameter can be mapped to the parameter T_0 (integration constant) that controls the diverging tachyon in the IR.

• There is also $x = \frac{N_f}{N_c}$ that has become continuous in the large N_c Veneziano limit.

Condensate dimension at the IR fixed point

• By expanding the DBI action we obtain the IR tachyon mass at the IR fixed point $\lambda = \lambda_*$ which gives the chiral condensate dimension:

$$-m_{\rm IR}^2 \ell_{\rm IR}^2 = \Delta_{\rm IR}(4 - \Delta_{\rm IR})$$

• Must reach the Breitenlohner-Freedman (BF) bound (horizontal line) at some x_c.

• x_c marks the *conformal phase transition*

Kaplan+Lee+Son+Stephanov

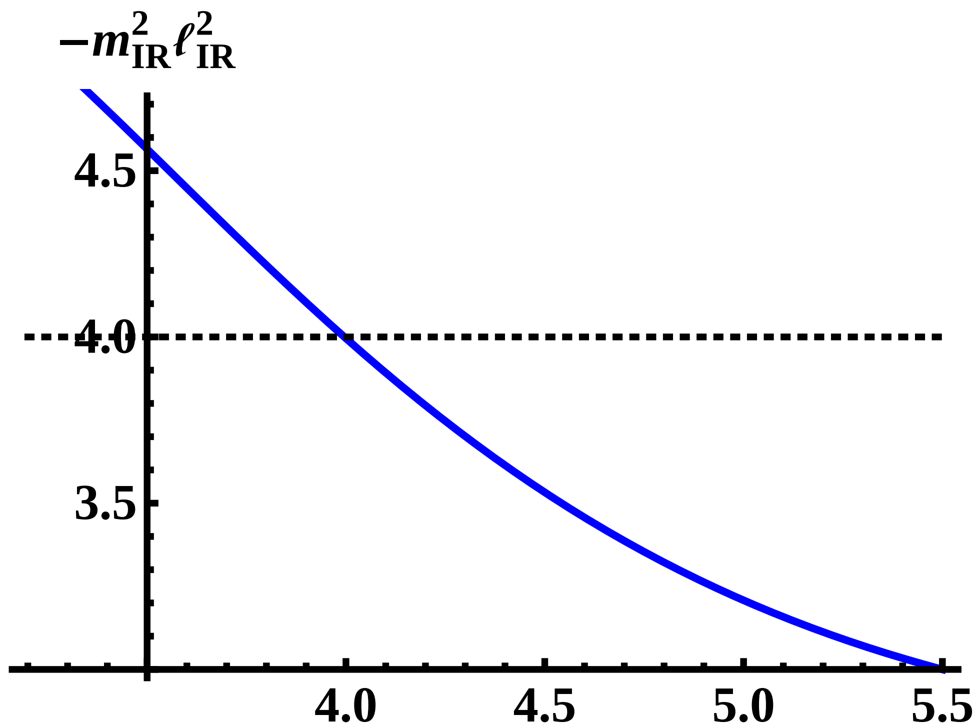

We obtain: $3.7 \lesssim x_c \lesssim 4.2$

UV mass vs IR parameter

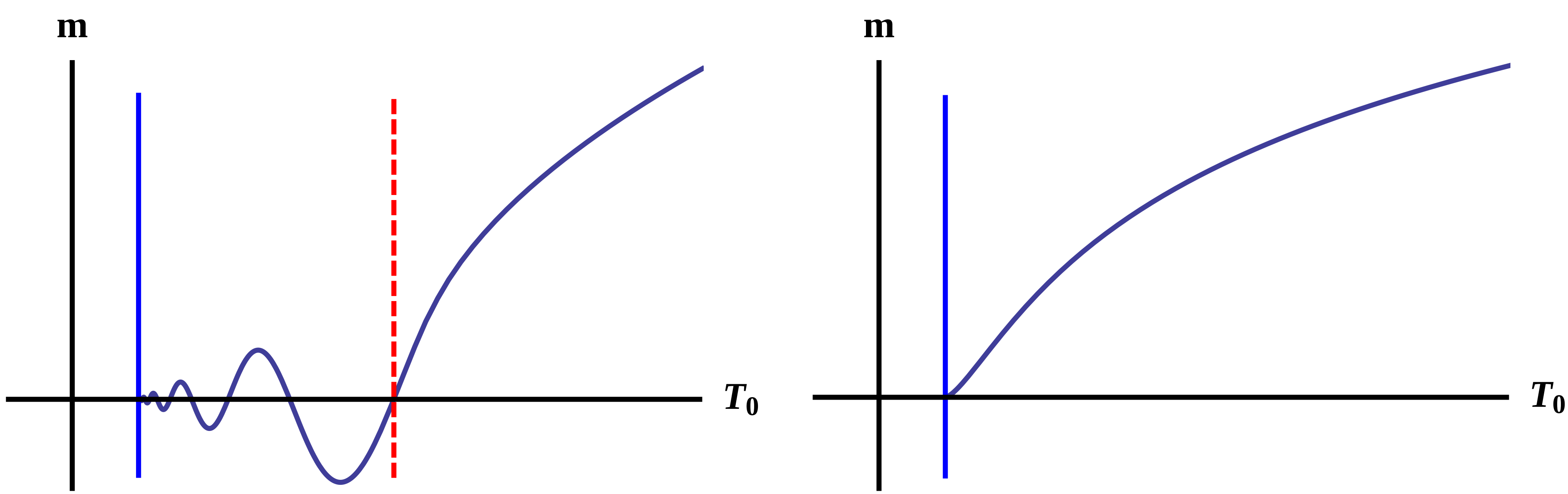

- Left figure: Plot of the UV Mass parameter m, as a function of the IR T_0 scale, for $x < x_c$. Right figure: Similar plot for $x \geq x_c$.

- At $m = 0$ there is an ∞ number of saddle point solutions (Efimov-like minima)

- The Efimov minima have free energies ΔE_n with

$$\Delta E_0 > \Delta E_1 > \Delta E_2 > \cdots$$

Efimov spiral

Ongoing work: $\sigma(m)$ dependence

- For $x < x_c$ spiral structure

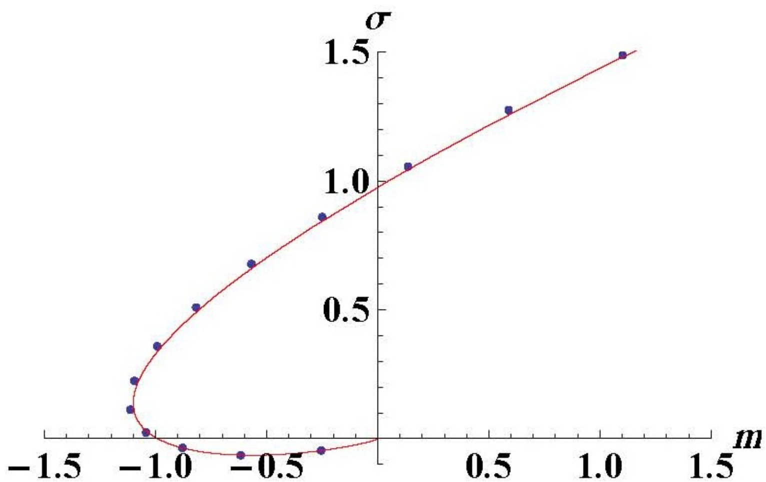

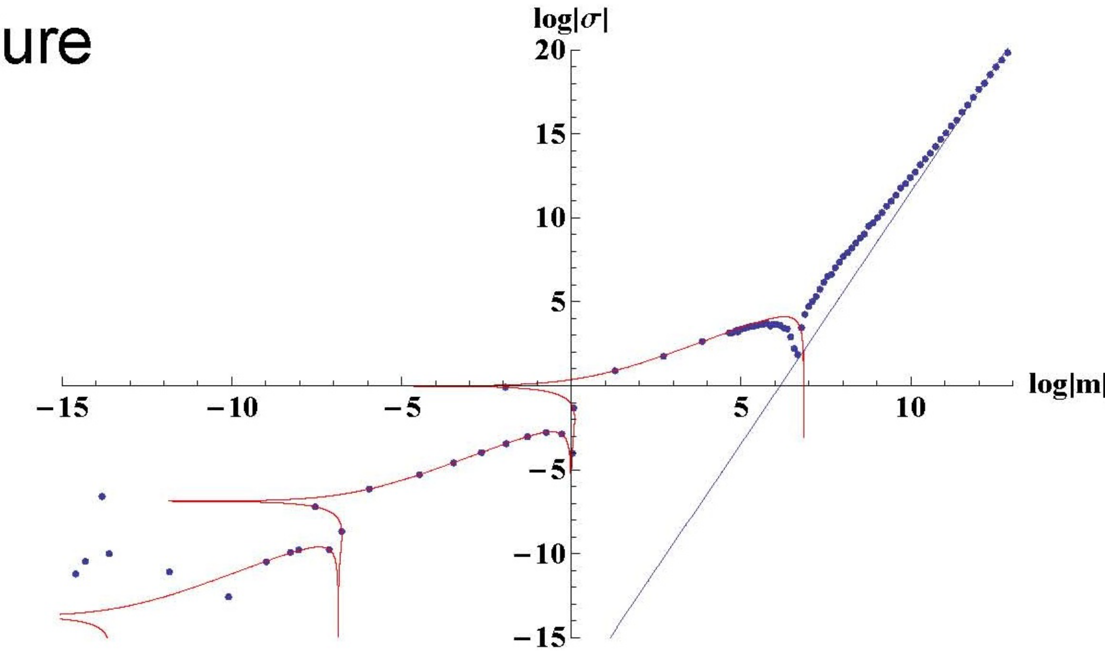

Walking

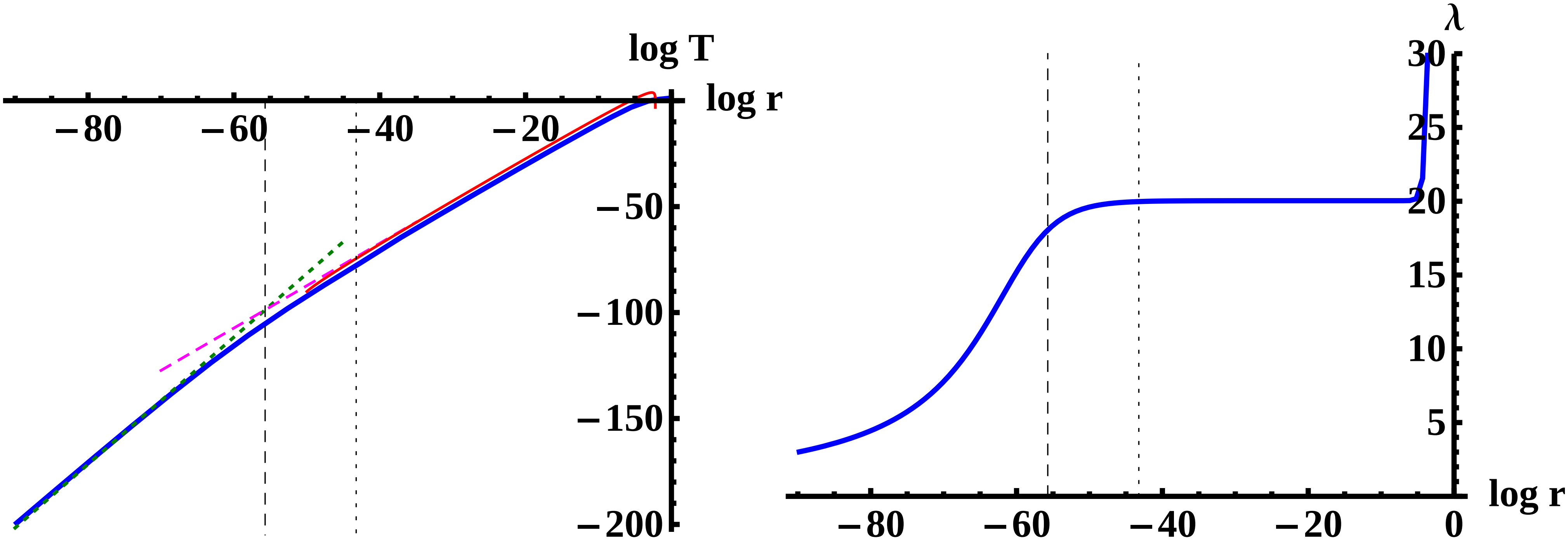

The tachyon $\log T$ (left) and the coupling λ (right) as functions of $\log r$ for an extreme walking background with $x = 3.992$. The thin lines on the left hand plot are the approximations used to derive the BKT scaling.

BKT/Miransky scaling

We obtain BKT-Miransky scaling:

$$\sigma \sim \Lambda_{\rm UV}^3 \ \exp\left(-\frac{2\hat{K}}{\sqrt{x_c - x}}\right) \ .$$

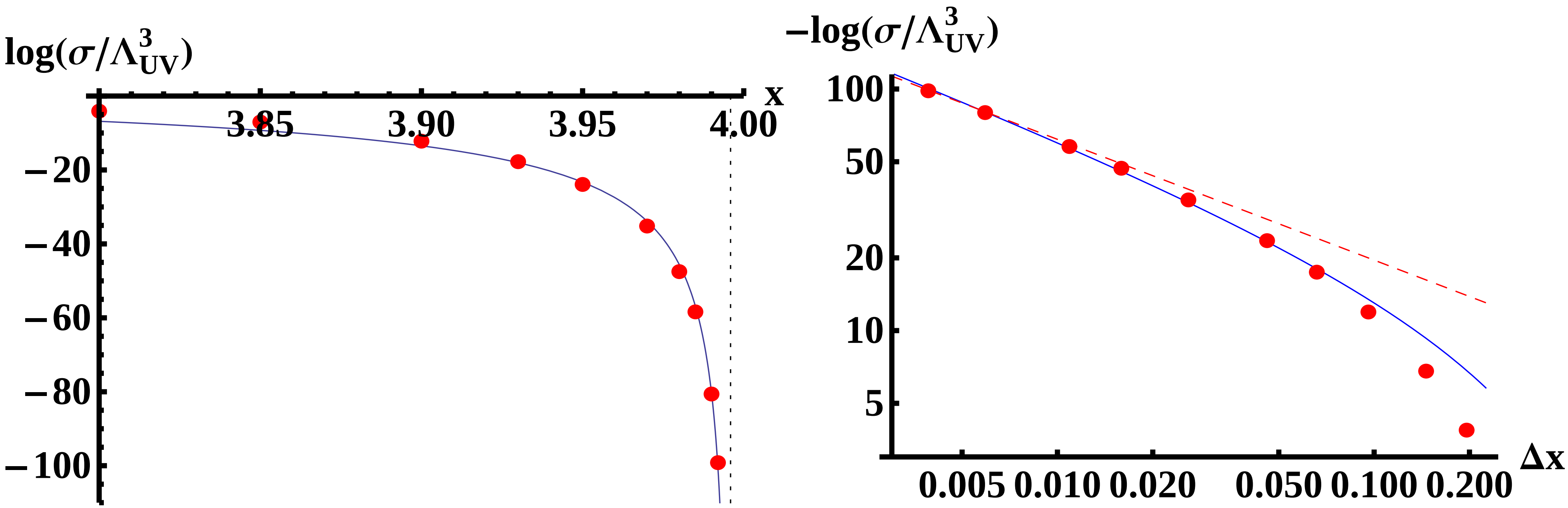

Left: $\log(\sigma/\Lambda^3)$ as a function of x (dots), compared to a BKT scaling fit (solid line). The vertical dotted line lies at $x = x_c$. Right: the same curve on log-log scale, using $\Delta x = x_c - x$.

Recap

- For $x = 0$, the theory has a mass gap, and confines.

- $0 < x < x_c \simeq 4$ the theory has chiral symmetry breaking, massless pions, and gapped spectrum otherwise.

- $x_c < x < \frac{11}{2}$ the theory is chirally symmetric, and flows to a non-trivial fixed point in the IR.

Spectra

• The main difference from all previous calculations is that here flavor back reacts on color.

• In the singlet sector the glueballs and mesons mix to leading order and the spectral problem becomes complicated.

• The conclusions are:

♠ All masses follow Miransky scaling in the walking region.

♠ There is no dilaton. Instead all (bound-state) masses go to zero exponentially fast.

♠ There are several level crossings as x varies but they seem accidental

♠ There is a subtle (and unexpected) discontinuity associated with the S-parameter.

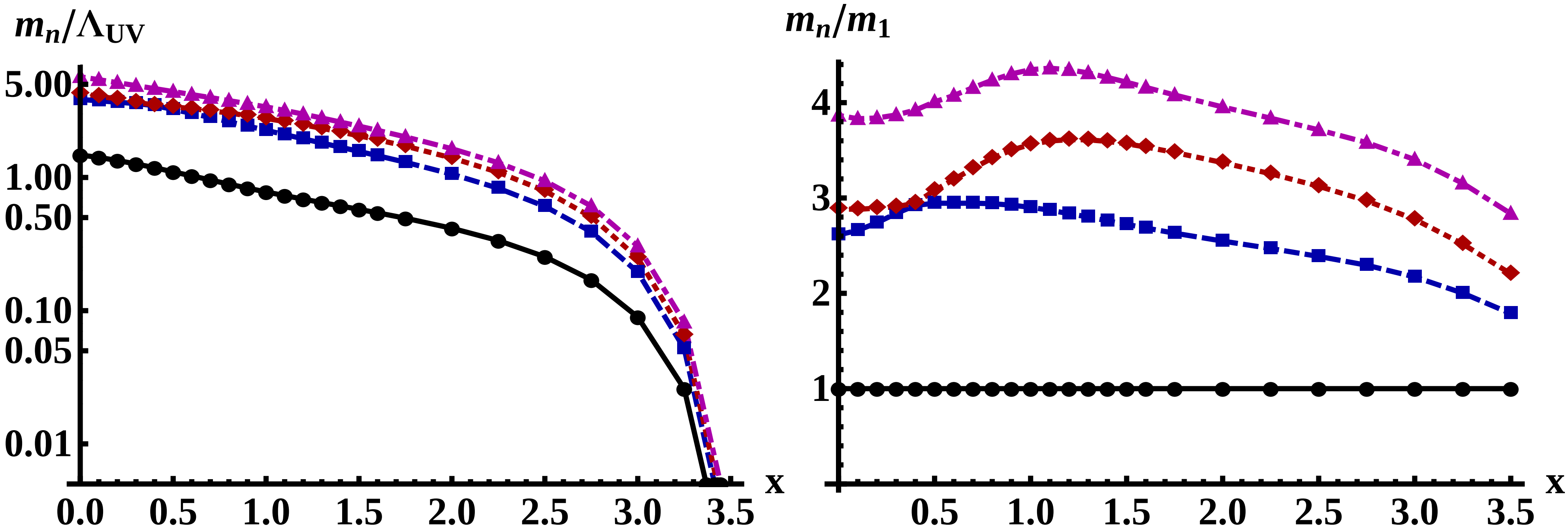

Singlet scalar meson spectra in the potential II class with SB normalization for W_0. They contain the 0^{++} glueballs and the singlet 0^{++} mesons that mix here at leading order. Left: the four lowest masses as a function of x in units of Λ_{UV}. Right: the ratios of masses of up to the fourth massive states as a function of x.

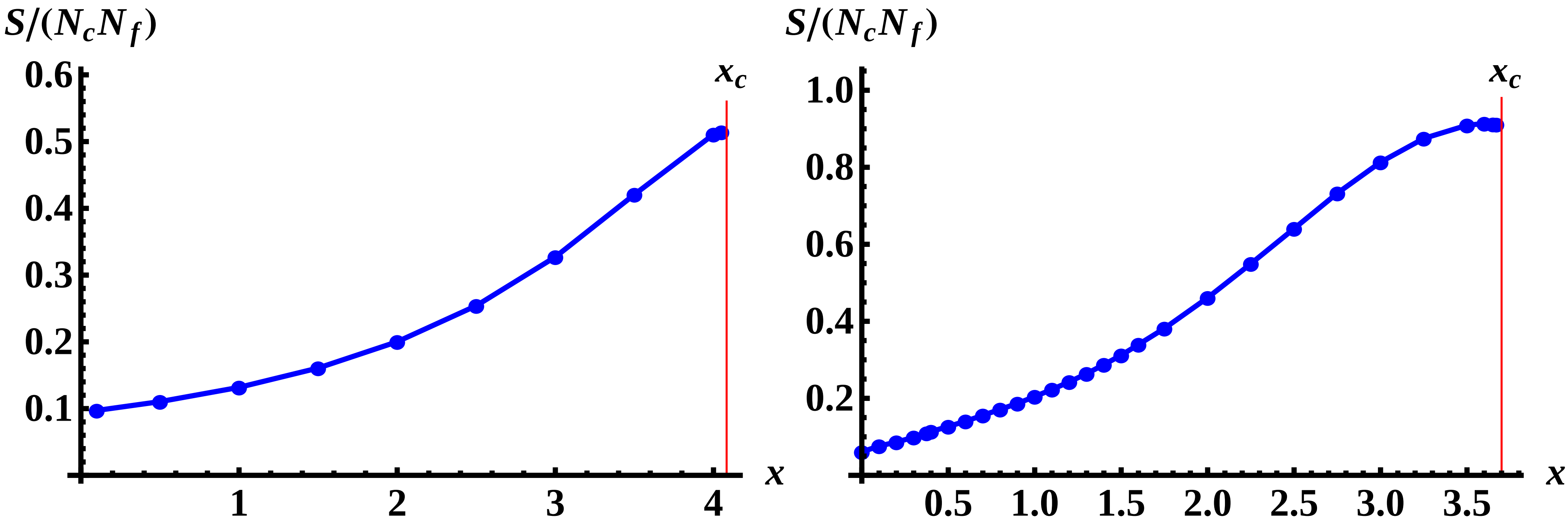

Left: The S-parameter as a function of x for potential class I with $W_0 = \frac{3}{11}$. Right: The S-parameter as a function of x for potential class II with SB normalization for W_0. In both cases S asymptotes to a finite value as $x \to x_c$.

Finite Temperature: the generic phase diagram

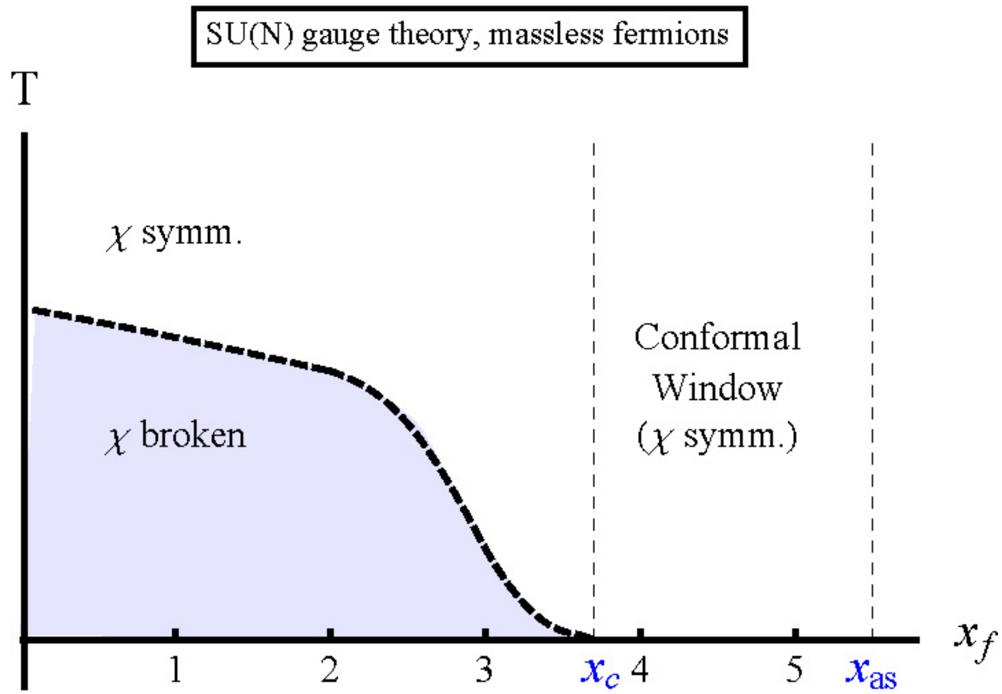

Qualitative behavior of the transition temperature between the low and high T phases of V-QCD matter.

- How is a deconfinement transition compete with the chiral transition?

- Are there further transitions (or crossovers) ?

The phase diagram

- It Depends on IR asymptotics. For QCD-like asymptotics it exhibits several transitions.

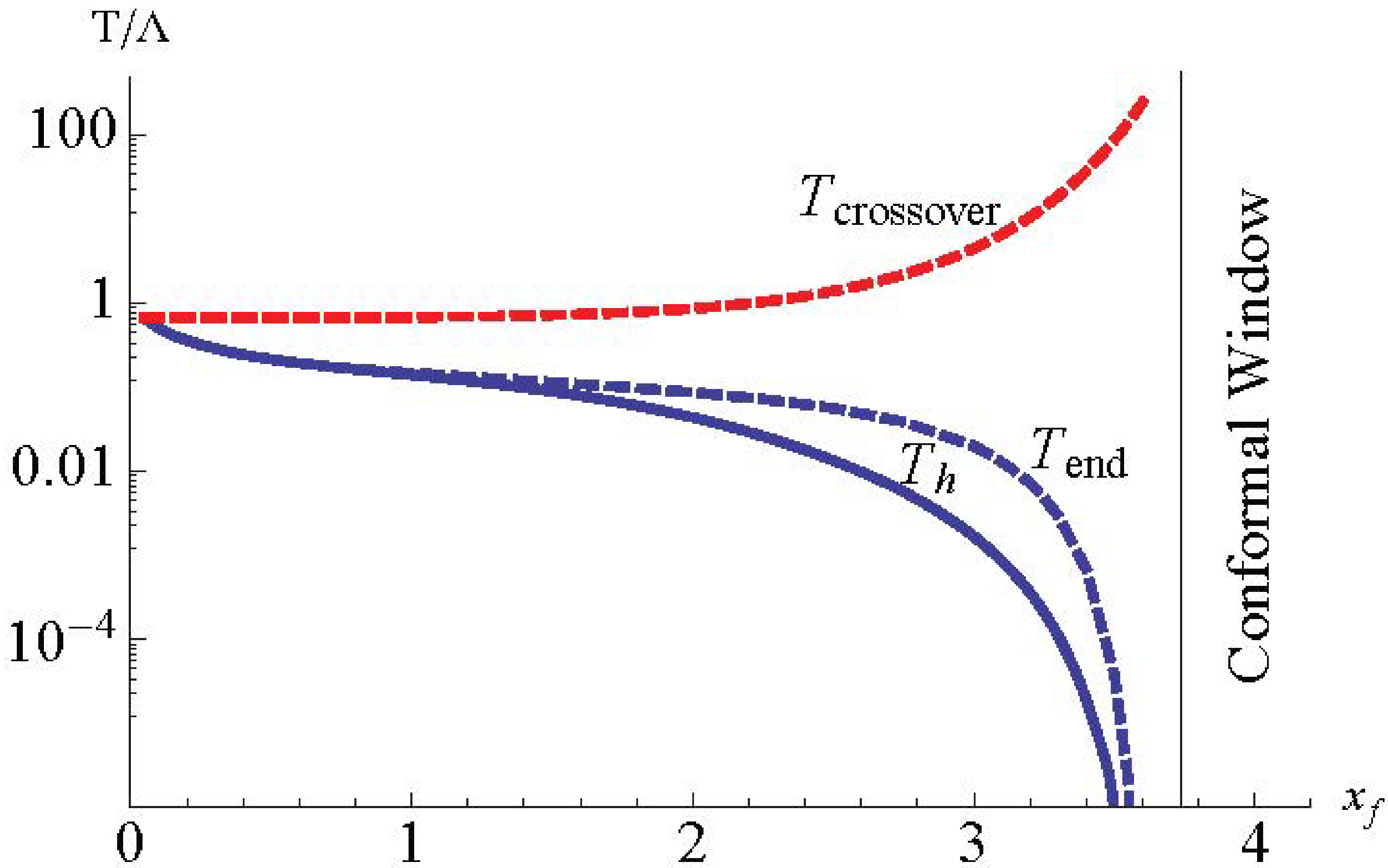

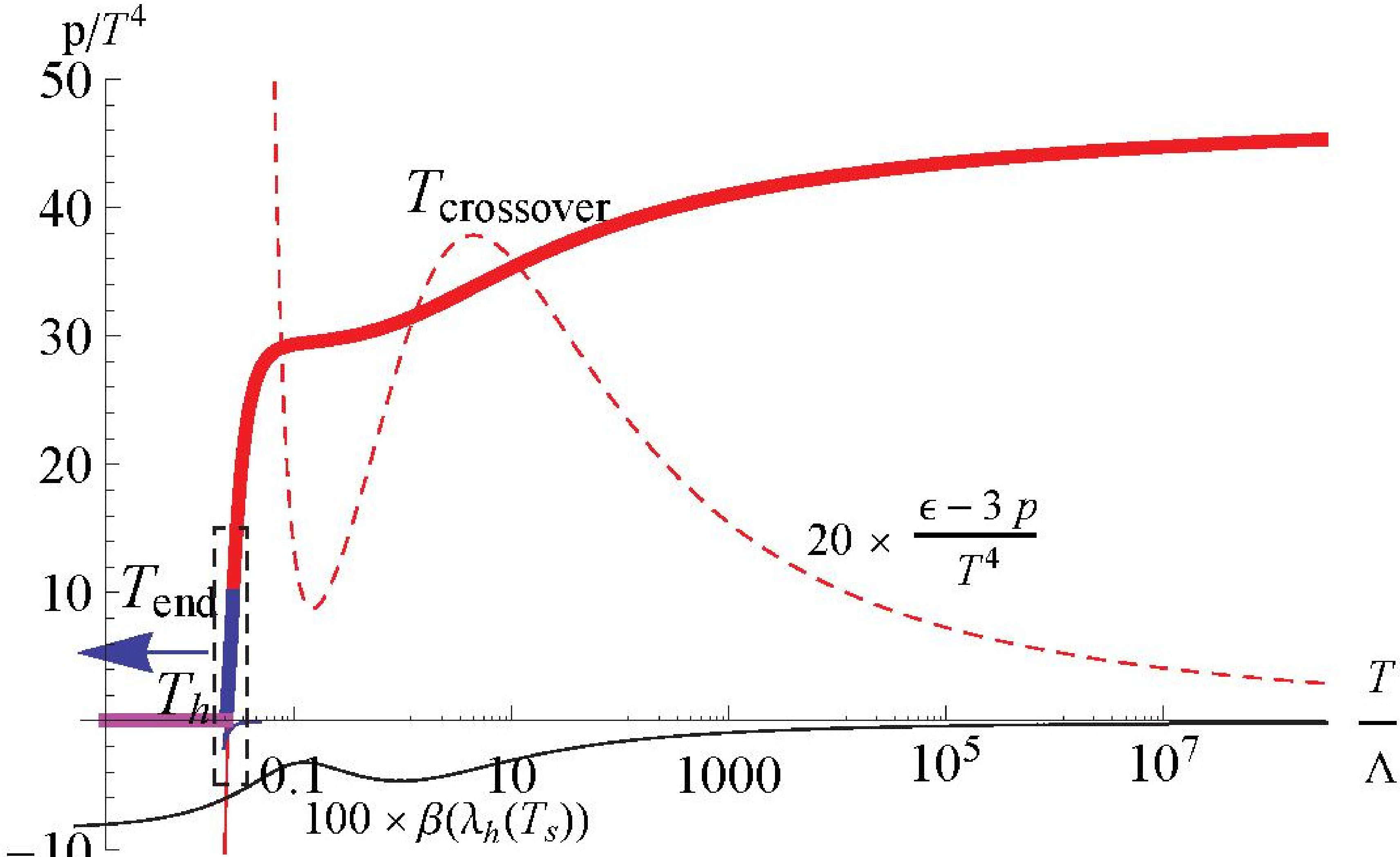

p/T^4
50
40
30
20
10
−10
$T_{crossover}$
$20 \times \frac{\epsilon - 3p}{T^4}$
T_{end}
T_h
0.1
10
1000
10^5
10^7
$100 \times \beta(\lambda_h(T_s))$
$\frac{T}{\Lambda}$

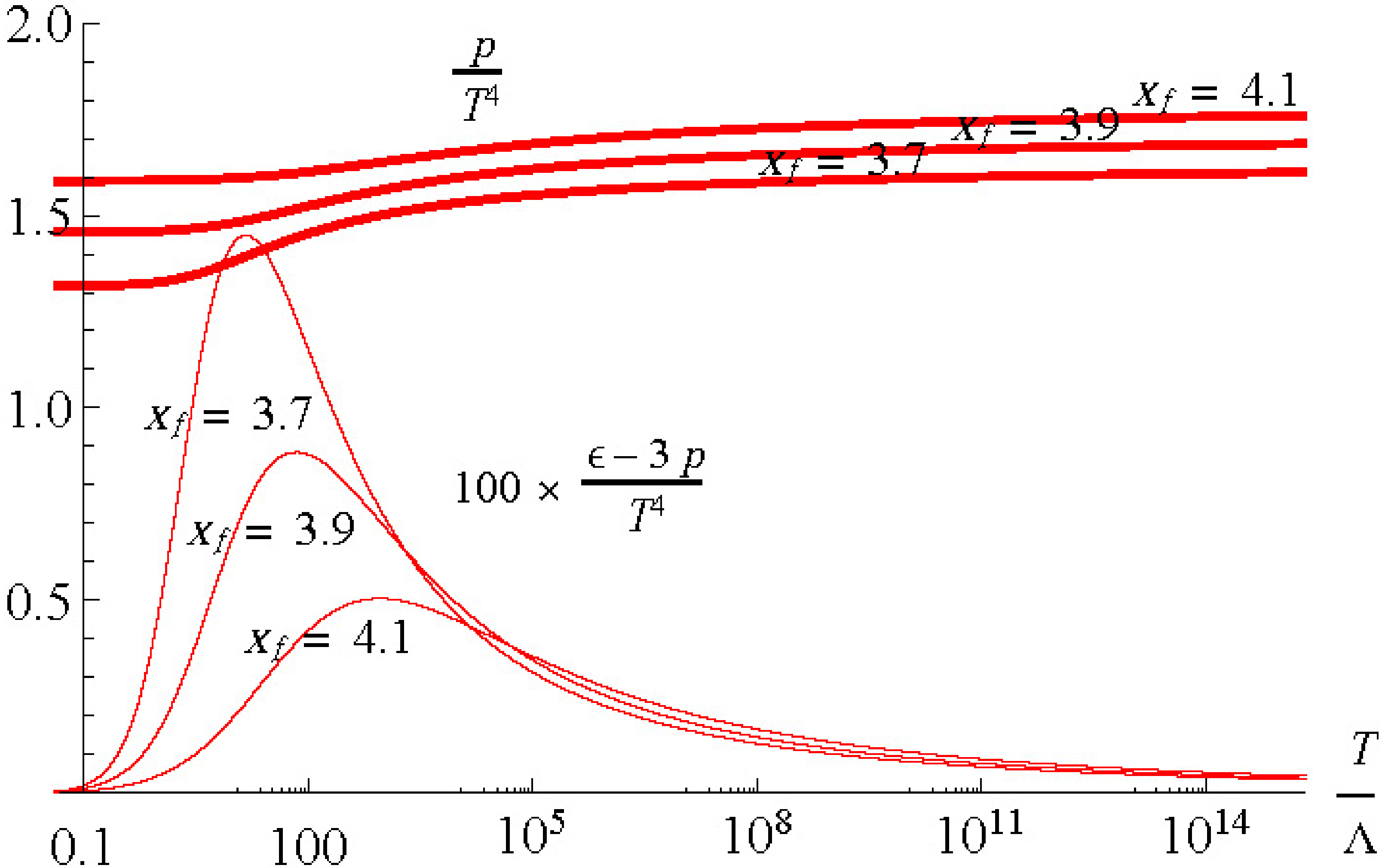
2.0
1.5
1.0
0.5
$\frac{p}{T^4}$
$x_f = 4.1$
$x_f = 3.9$
$x_f = 3.7$
$x_f = 3.7$
$x_f = 3.9$
$x_f = 4.1$
$100 \times \frac{\epsilon - 3p}{T^4}$
0.1
100
10^5
10^8
10^{11}
10^{14}
$\frac{T}{\Lambda}$

The phase structure at finite density: background

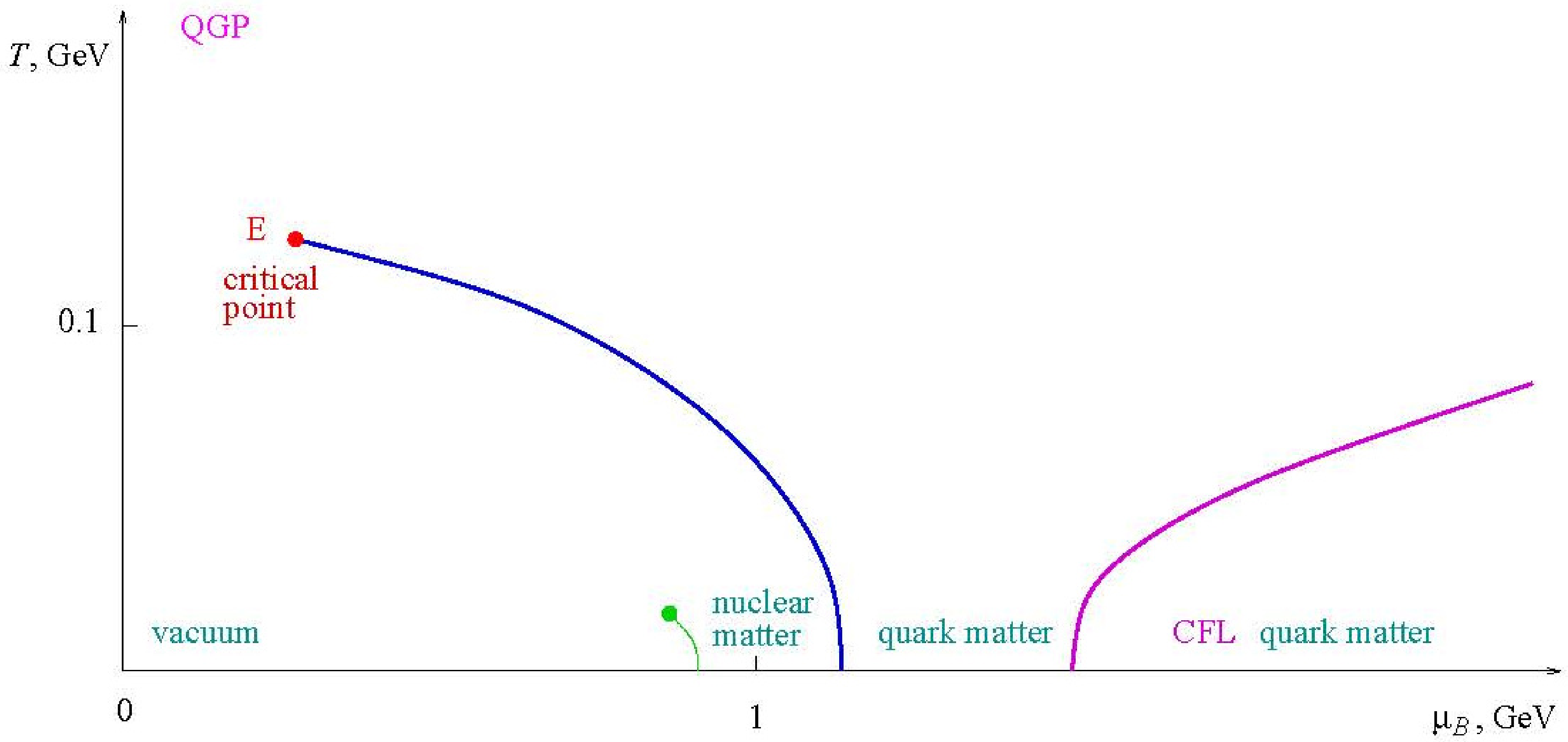

from Stephanov review, '04

• First principle techniques like lattice are not very useful as the Monte Carlo probability measure is complex at finite μ.

• Various tricks have been tried (lattice re-weighting, resuming μ-moments). Difficult to assess.

• Phenomenological models have been also used: NJL(+Polyakov), Random Matrix, Linear sigma models, Statistical bootstrap models, effective potential (CJT) models, composite operators, etc. suggesting the diagram above.

• We would like to investigate the same question using the V-QCD holographic model.

• We take massless quarks, and $x = 1$ ($N_f = N_c = \infty$).

• Our results are preliminary and the model is not perfectly tuned to QCD.

The phase structure at finite density

- The rough phase diagram.

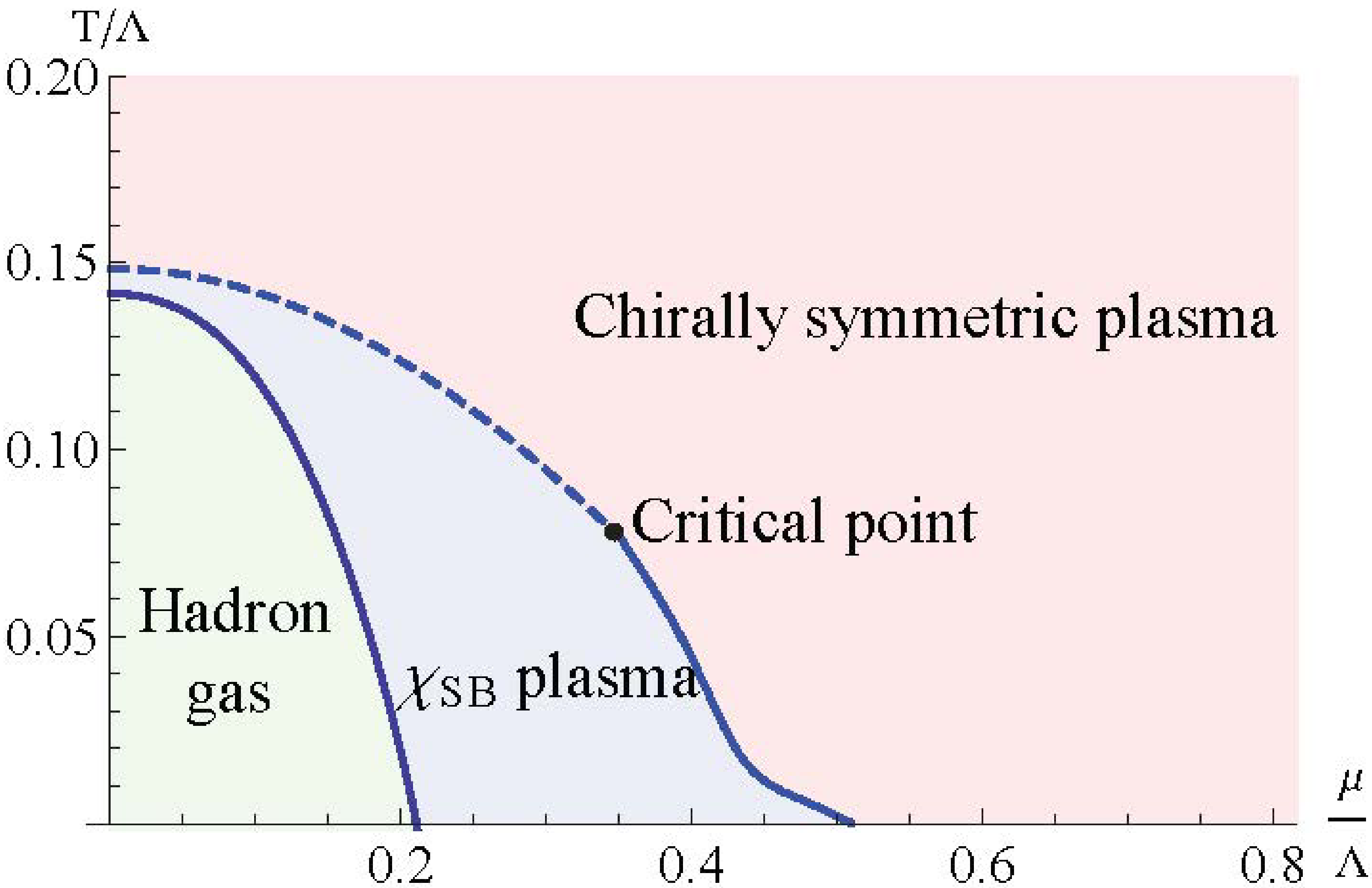

There are two quantum critical first order phase transitions.

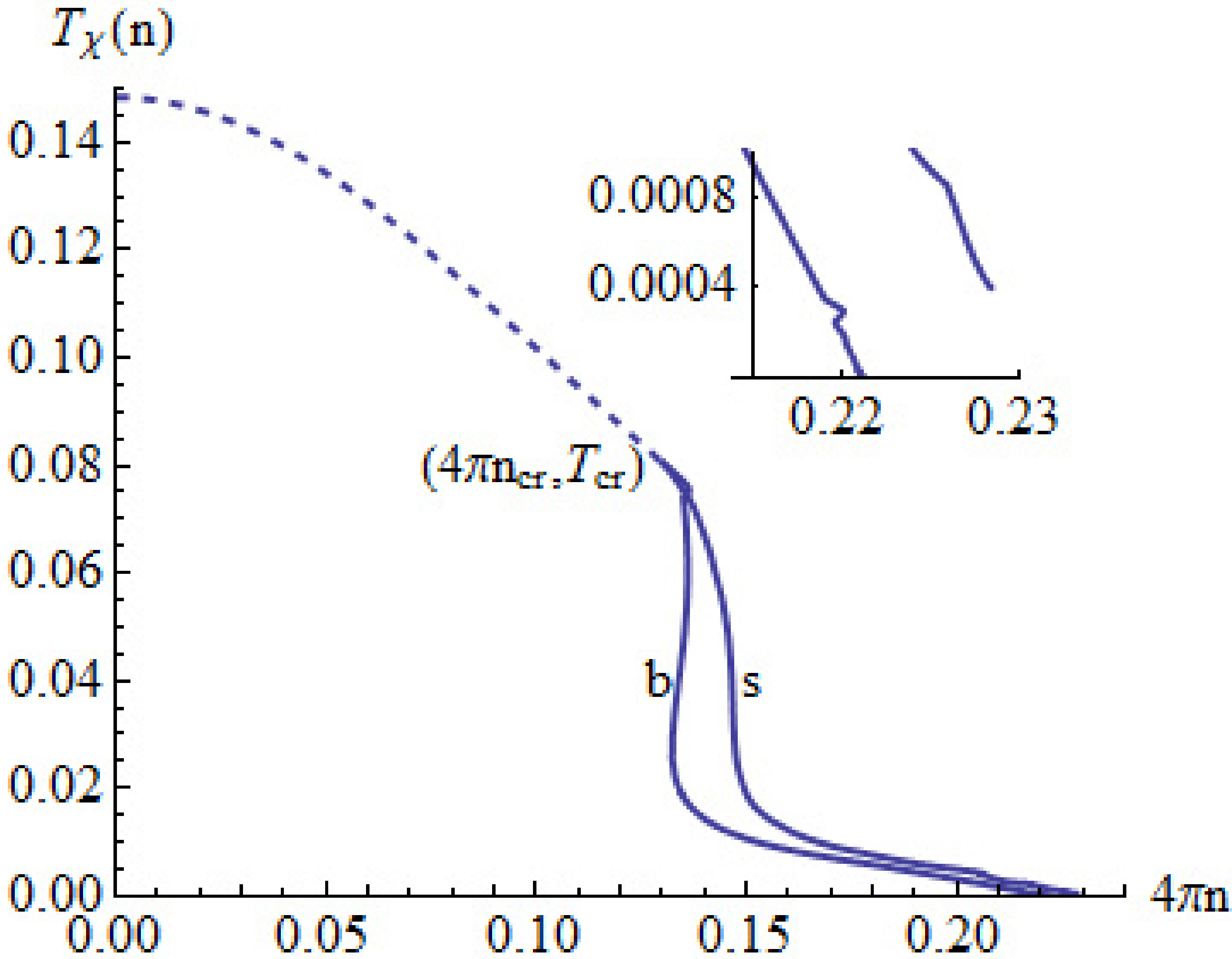

Dependence of the chiral transition temperature on chemical potential or on quark number density. Along the 1st order line there is a jump in n. The inset shows a closeup of the $T = 0$ region with density jump. The hadronic phase has been "squeezed on the $n = 0$ axis.

A new quantum critical regime

• The most remarkable new feature is a new quantum critical regime at $T = 0$ and finite μ.

• This is clear in the (cold) quark gluon plasma phase at $\mu/\Lambda > 0.5$.

• It seems also to be present in the chirally-broken plasma phase but our numerics are not yet good enough to be sure.

• This is a phase with a $AdS_2 \times R^3$ geometry as in the RN black hole. Spacial points cannot communicate, it is like the speed of light is equal to 0.

• Such critical points are highly unstable, and are expected to give rise to superconducting states.

Outlook

• We have analyzed holographic theories that share many features with QCD in the Veneziano limit.

• We have characterized the landscape and $T = 0$ phase diagram of such theories based both on first principles from string theory and phenomenological input.

• We have also analyzed the finite T phase diagrams and their spectra and we started the study of their finite density behavior.

• We have found that the long sought dilatons and vanishing S-parameters are inexistant in this class.

There are several shortcomings that should be addressed:

• Control the quantum corrections of the holographic fields that are not suppressed. They are expected to affect the behavior in some regimes of the phase diagram.

• At sufficiently high density, point-like baryons will populate the plasma (holographic flavor instantons). This is a very difficult system to handle.

• A more precise contact with string theory would be welcome.

Immediate directions that remain to be explored:

- Construct a detailed holographic model that reproduces known quantitative features of QCD.

- Study energy loss of quarks in QGP (with full backreaction).

- Continue and complete the phase diagram at finite density.

- Study transport and hydrodynamics in the walking region.

- Addition of multi-trace operators of the quark mass operators. These affect the walking region, rearrange the Efimov vacua, and are generated in technicolor setups.

- The physics in the walking region resembles the zero tension limit of string theory. Can we learn something more here?

Bibliography

Based on recent work with:

Matti Jarvinnen (Crete) arXiv:1112.1261 [hep-ph]

T. Alho (Helsinki), M. Jarvinnen (Crete), K. Kajantie (Helsinki), K. Tuominnen (Helsinki).
arXiv: 1210.4516 [hep-ph]

- D. Arean (SISSA) I. Iatrakis, (Crete), M. Jarvinnen (Crete)
arXiv:1211.6125 [hep-ph] arXiv:1309.2286 [hep-ph]

- T. Alho (Helsinki), M. Jarvinnen (Crete), K. Kajantie (Helsinki), C. Rosen (Crete), K. Tuominnen (Helsinki). To appear soon.

and past work with:

- A. Paredes (Barcelona), I. Iatrakis, (Crete)

arXiv:1003.2377 [hep-ph] ; arXiv:1010.1364 [hep-ph]

.

Thank you

This research has been co-financed by the European Union (European Social Fund, ESF) and Greek national funds through the Operational Program "Education and Lifelong Learning" of the National Strategic Reference Framework (NSRF), under the grants schemes "Funding of proposals that have received a positive evaluation in the 3rd and 4th Call of ERC Grant Schemes" and the program "Thales"

European Union
European Social Fund

OPERATIONAL PROGRAMME
EDUCATION AND LIFELONG LEARNING
investing in knowledge society
MINISTRY OF EDUCATION & RELIGIOUS AFFAIRS, CULTURE & SPORTS
MANAGING AUTHORITY

NSRF
2007-2013
programme for development
EUROPEAN SOCIAL FUND

Co-financed by Greece and the European Union

N=1 sQCD

The case of $\mathcal{N} = 1$ $SU(N_c)$ superQCD with N_f quark multiplets is known and provides an interesting (although much more complex) example for the non-supersymmetric case.

Seiberg

• $x = 0$ the theory has confinement, a mass gap and N_c distinct vacua associated with a spontaneous breaking of the leftover R symmetry Z_{N_c}.

• At $0 < x < 1$, the theory has a runaway ground state.

• At $x = 1$, the theory has a quantum moduli space with no singularity. This reflects confinement with χSB.

• At $x = 1 + \frac{1}{N_c}$, the moduli space is classical (and singular). The theory confines, but there is no χSB.

• At $1+\frac{2}{N_c} < x < \frac{3}{2}$ the theory is in the non-abelian magnetic IR-free phase, with the magnetic gauge group $SU(N_f - N_c)$ IR free.

• At $\frac{3}{2} < x < 3$, the theory flows to a CFT in the IR. (conformal window)

Near $x = 3$ this is the Banks-Zaks region where the original theory has an IR fixed point at weak coupling. Moving to lower values, the coupling of the IR $SU(N_c)$ gauge theory grows.

However near $x = \frac{3}{2}$ the dual magnetic $SU(N_f - N_c)$ is in its Banks-Zaks region, and provides a weakly coupled description of the IR fixed point theory.

• At $x > 3$, the theory is IR free.

Below the BF bound

• Correlation of the violation of BF bound and the conformal phase transition

• For $\Delta_{\text{IR}}(4-\Delta_{\text{IR}})<4$

$$T(r) \sim m_q r^{4-\Delta_{\text{IR}}} + \sigma r^{\Delta_{\text{IR}}}$$

• For $\Delta_{\text{IR}}(4-\Delta_{\text{IR}})>4$

$$T(r) \sim C r^2 \sin\left[(\text{Im}\Delta_{\text{IR}})\log r + \phi\right]$$

Two possibilities:

• $x > x_c$: BF bound satisfied at the fixed point $\Rightarrow$ only trivial massless solution ($T \equiv 0$, ChS intact, fixed point hit)

• $x < x_c$: BF bound violated at the fixed point $\Rightarrow$ a nontrivial massless solution exists, which drives the system away from the fixed point.

Conclusion: *phase transition* at $x = x_c$

Matching to QCD

- $V_g(\lambda)$ is fixed from glue.

- The UV is adjusted to perturbative QCD.

$$V_g \sim V_0 + \mathcal{O}(\lambda) \quad , \quad V_0 \sim W_0 + \mathcal{O}(\lambda)$$

$$V_0 - xW_0 = \frac{12}{\ell_{UV}^2}$$

- W_0 is one of the most important parameters of the models.

• There are two classes of tachyon potentials:

♠ Type I: $T \sim e^{Cr}$ as $r \to \infty$.

♠ Type II $T \sim \sqrt{r}$ as $r \to \infty$.

• In all cases the "regular" IR solution depends on a single undetermined constant (instead on two).

• The phase structure is essentially independent of IR choices.

Varying the model

"prediction" for x_c

After fixing UV coefficients from QCD, there is still freedom in choosing the leading coefficient of V_0 at $\lambda \to 0$ and the IR asymptotics of the potentials

Thick blue $\to V_I$

Thin red $\to V_{II}$

Resulting variation of the edge of conformal window

$3.7 \lesssim x_c \lesssim 4.2$

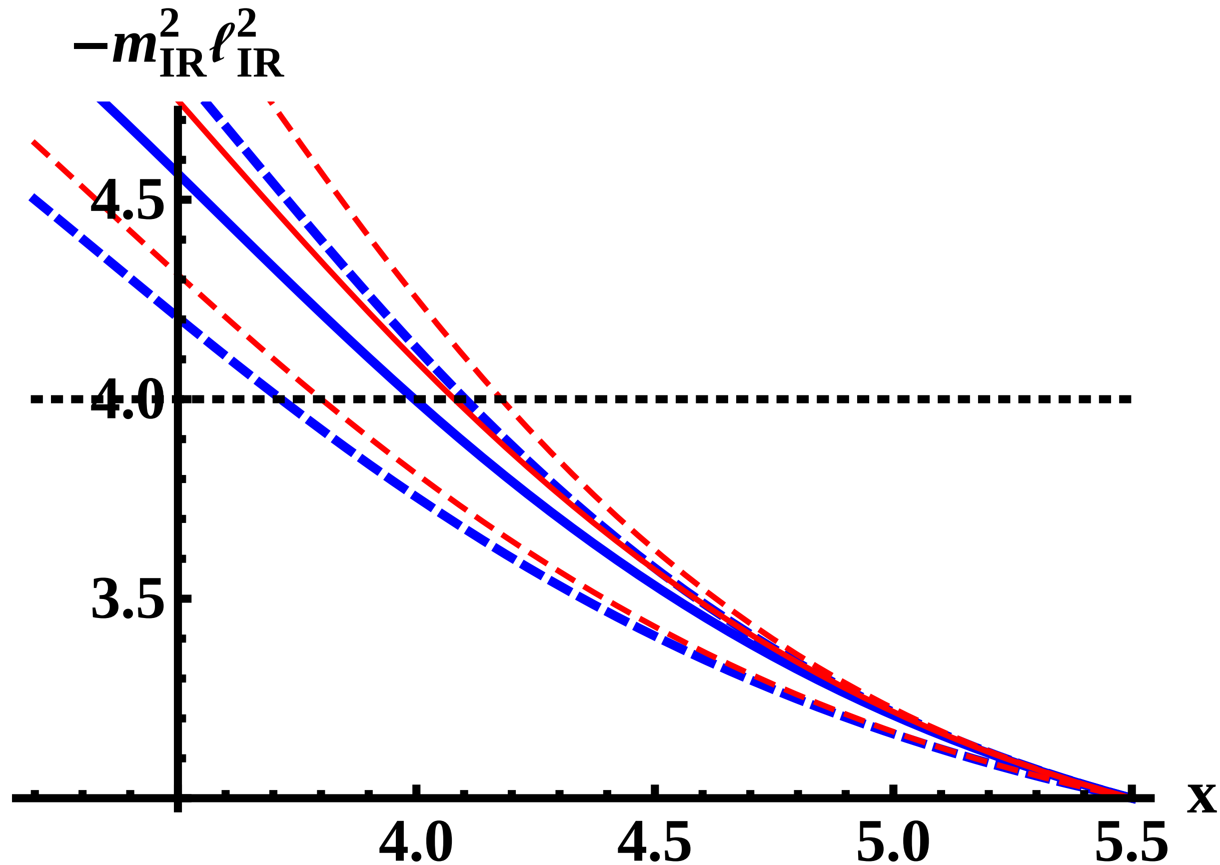

RETURN

The IR fixed point

$$V_{\text{eff}}(\lambda) = V_g(\lambda) - xV_0(\lambda)$$

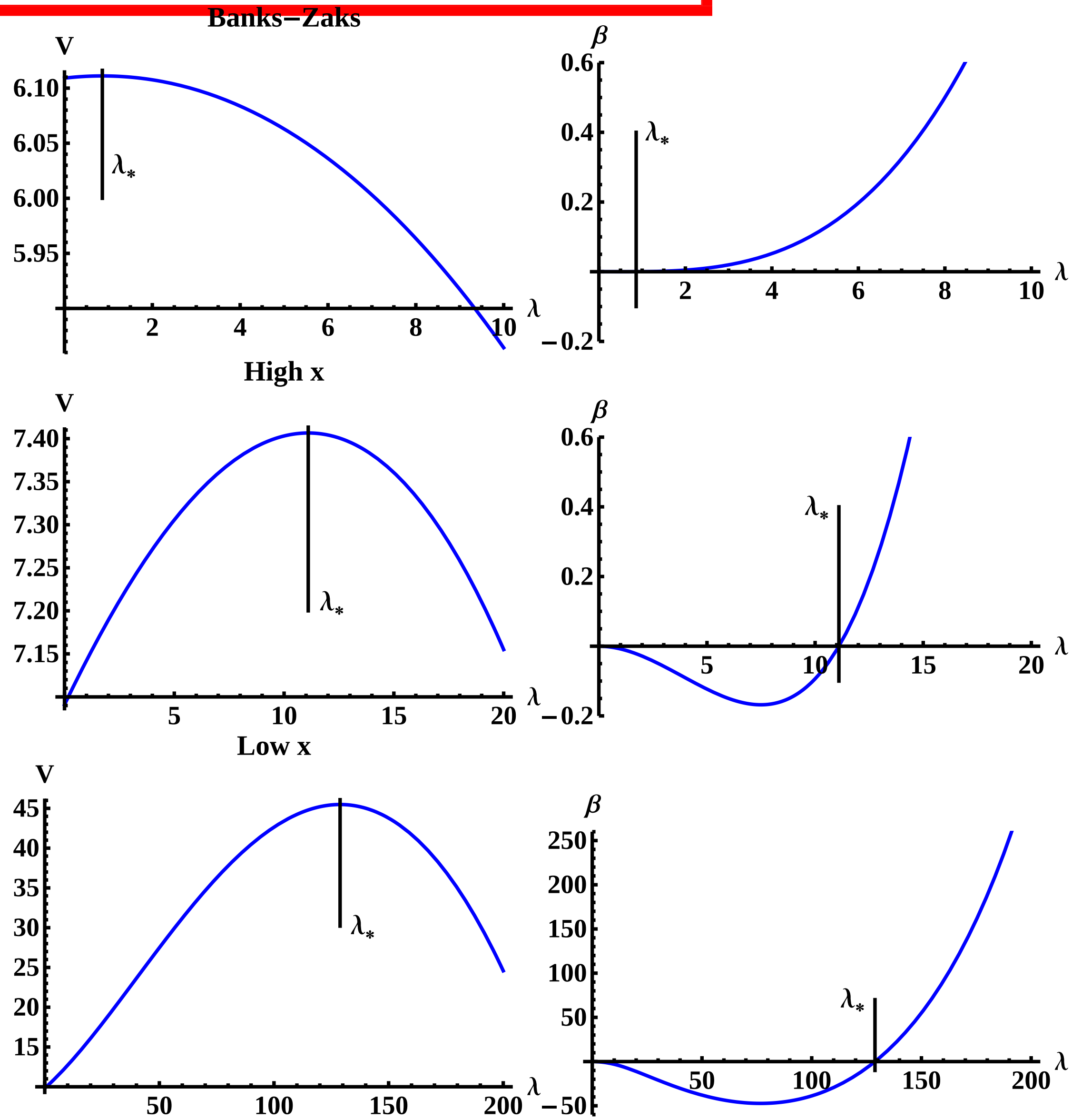

Two possibilities: (a) The maximum exists for all x. (b) The maximum exists for $x > x_*$.

Matching to QCD: UV

• As $\lambda \to 0$ we can match:

♠ $V_g(\lambda)$ with (two-loop) Yang-Mills β-function.

♠ $V_g(\lambda) - xV_0(\lambda)$ with QCD β-function.

♠ $a(\lambda)/h(\lambda)$ with anomalous dimension of the quark mass/chiral condensate

• The matching allows to mark the BZ point, that we normalize at $x = \frac{11}{2}$.

• After the matching above we are left with a single undetermined parameter in the UV:

$$V_g \sim V_0 + \mathcal{O}(\lambda) \quad , \quad V_0 \sim W_0 + \mathcal{O}(\lambda)$$

$$V_0 - xW_0 = \frac{12}{\ell_{UV}^2}$$

Matching to QCD: IR

• In the IR, the tachyon has to diverge $\Rightarrow$ the tachyon action $\propto e^{-T^2}$ becomes small

♠ $V_g(\lambda) \simeq \lambda^{\frac{4}{3}}\sqrt{\lambda}$ chosen as for Yang-Mills, so that a "good" IR singularity exists etc.

♠ $V_0(\lambda)$, $a(\lambda)$, and $h(\lambda)$ chosen to produce tachyon divergence: there are several possibilities.

♠ The phase structure is essentially independent of IR choices.

Choice I, for which in the IR

$$T(r) \sim T_0 \exp\left[\frac{81\ 3^{5/6}(115-16x)^{4/3}(11-x)}{812944\ 2^{1/6}}\frac{r}{R}\right] \quad , \quad r \to \infty$$

R is the IR scale of the solution. T_0 is the control parameter of the UV mass.

Choice II: for which in the IR

$$T(r) \sim \frac{27\ 2^{3/4}3^{1/4}}{\sqrt{4619}}\sqrt{\frac{r-r_1}{R}} \quad , \quad r \to \infty$$

R is the IR scale of the solution. r_1 is the control parameter of the UV mass.

The free energy

The free energy difference between the ChS and ChSB $m_q = 0$ solutions

Chiral symmetry breaking solution favored whenever it exists ($x < x_c$)

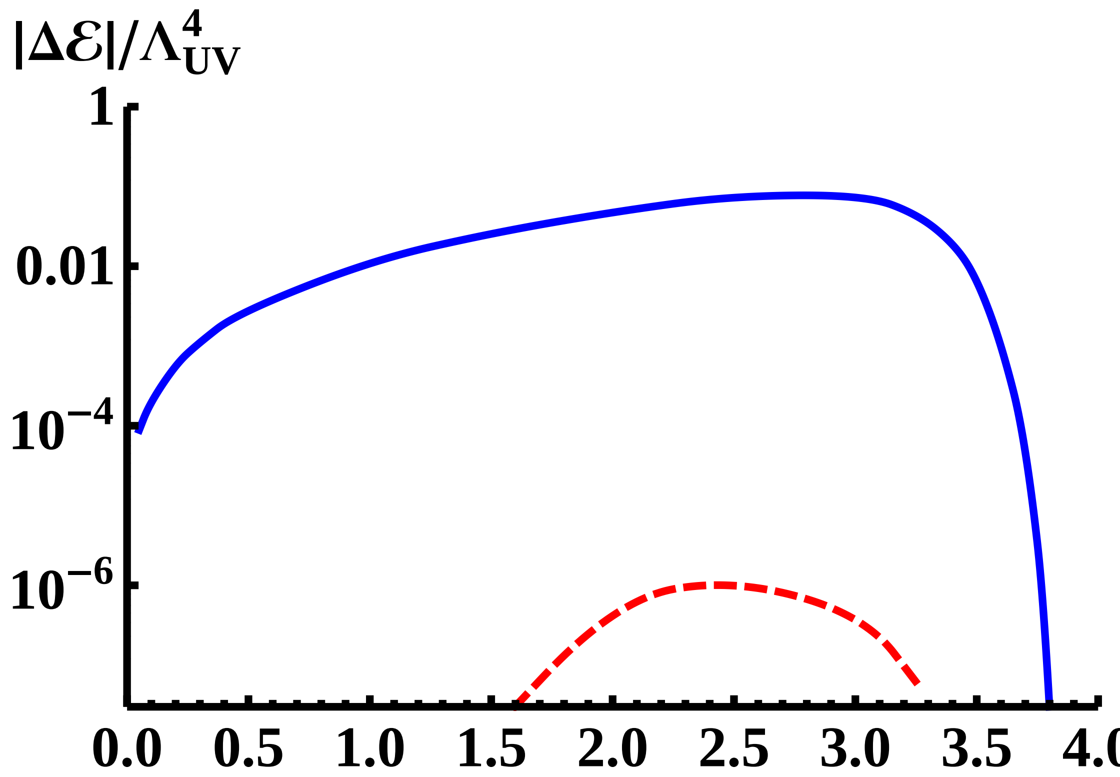

- The Efimov minima have free energies ΔE_n with

$$\Delta E_0 > \Delta E_1 > \Delta E_2 > \cdots$$

Walking

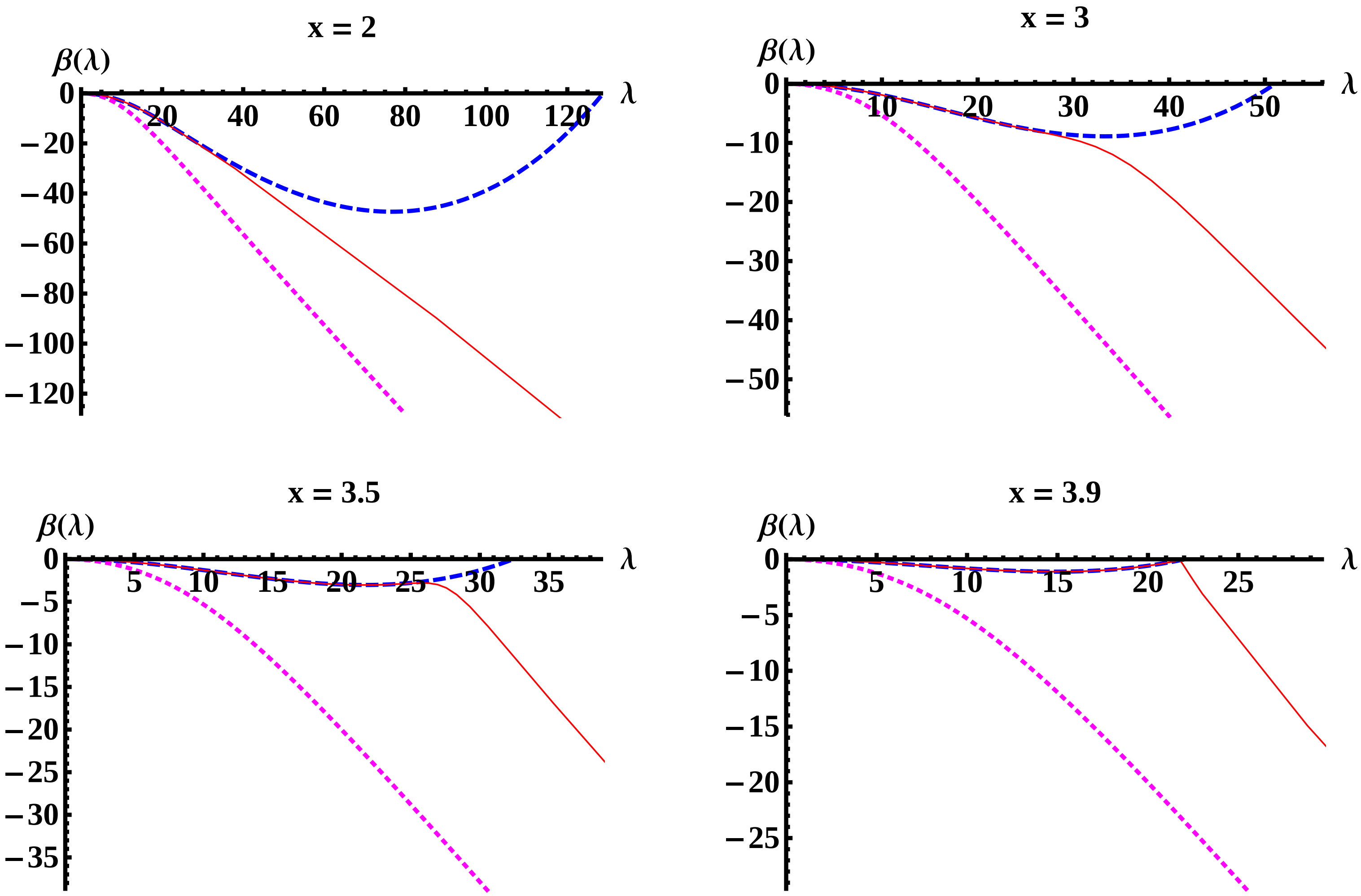

The β-functions for vanishing quark mass for various values of x. The red solid, blue dashed, and magenta dotted curves are the β-functions corresponding to the full numerical solution $(d\lambda/dA)$ along the RG flow, the potential $V_{\text{eff}} = V_g - xV_{f0}$, and the potential V_g, respectively.

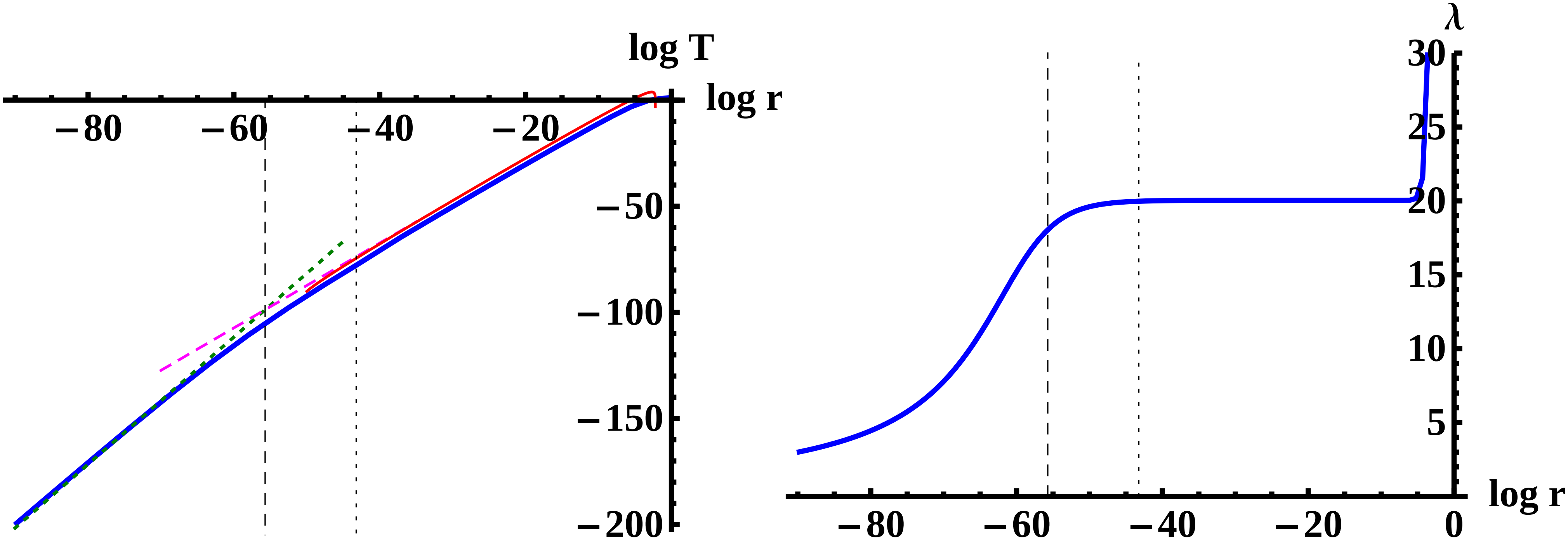

The tachyon $\log T$ (left) and the coupling λ (right) as functions of $\log r$ for an extreme walking background with $x = 3.992$. The thin lines on the left hand plot are the approximations used to derive the BKT scaling.

Holographic β-functions

The second order equations for the system of two scalars plus metric can be written as first order equations for the β-functions

Gursoy+Kiritsis+Nitti

$$\frac{d\lambda}{dA} = \beta(\lambda, T) \quad , \quad \frac{dT}{dA} = \gamma(\lambda, T)$$

The equations of motion boil down to two partial non-linear differential equations for β, γ.

Such equations have also branches as for DBI and non-linear scalar actions the relation of $e^{-A}A'$ with the potentials is a polynomial equation of degree higher than two.

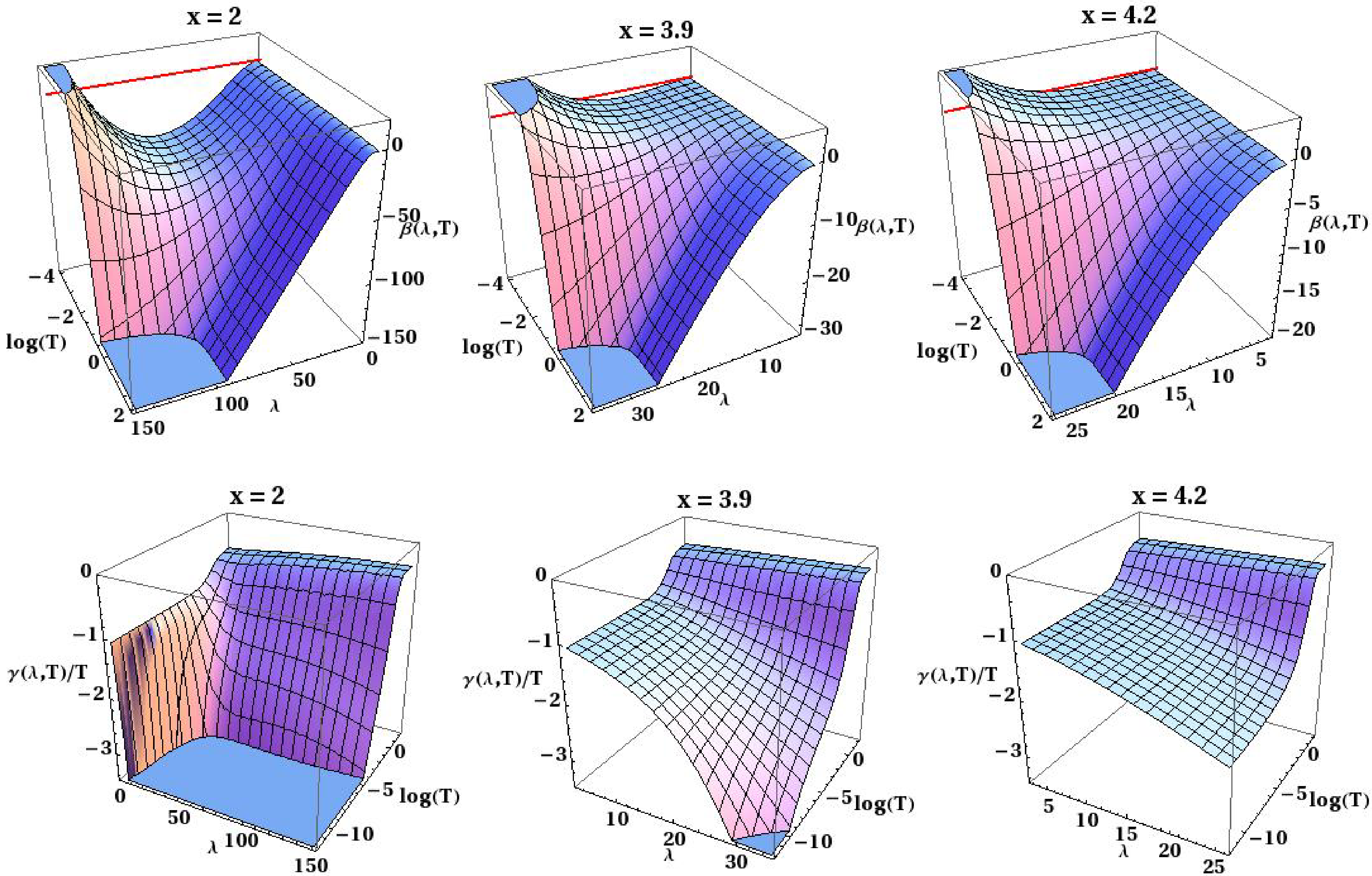

The red lines are added on the top row at $\beta = 0$ in order to show the location of the fixed point.

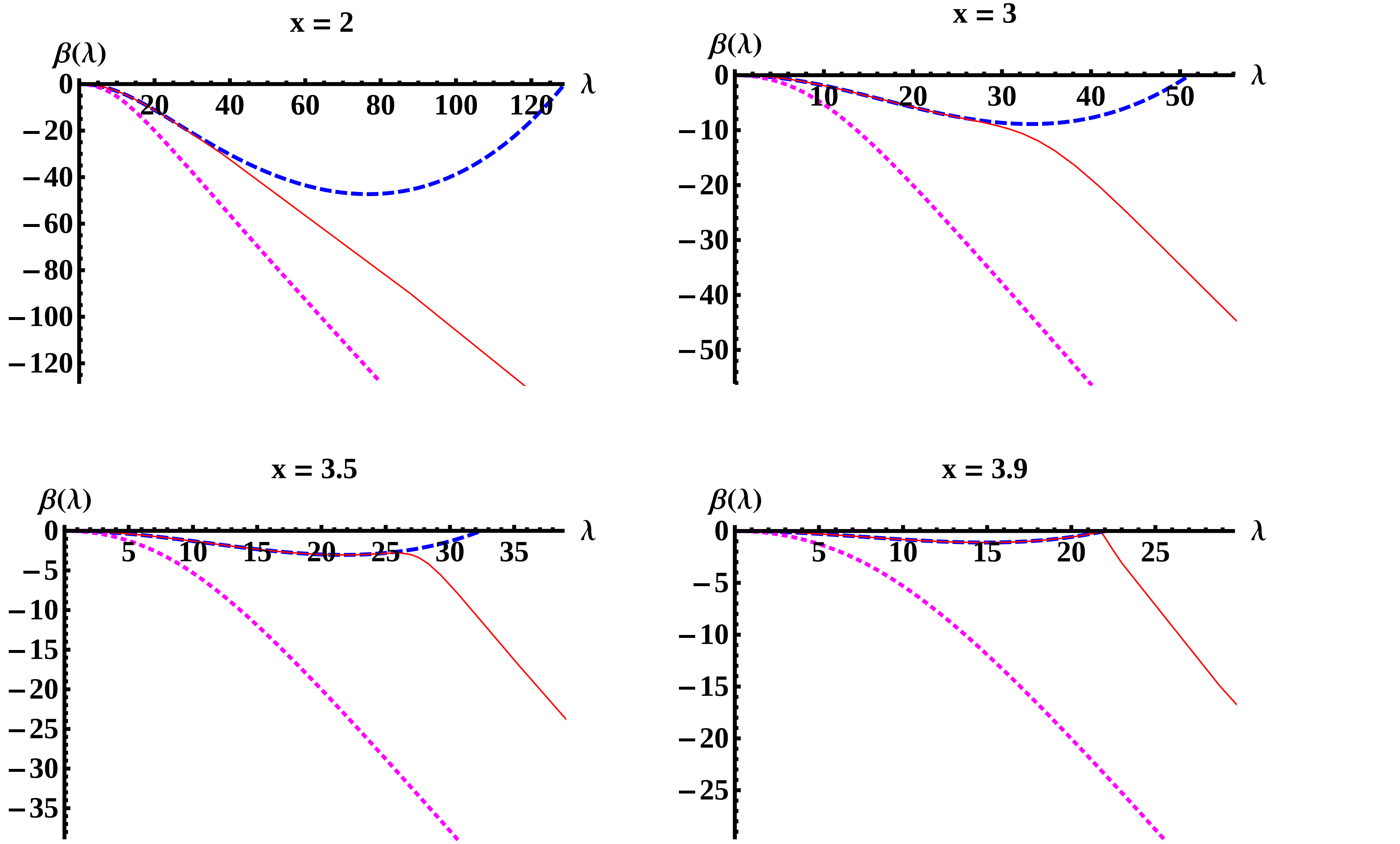

The β-functions for vanishing quark mass for various values of x. The red solid, blue dashed, and magenta dotted curves are the β-functions corresponding to the full numerical solution ($d\lambda/dA$) along the RG flow, the potential $V_{\text{eff}} = V_g - xV_{f0}$, and the potential V_g, respectively.

UV mass vs T_0 and r_1

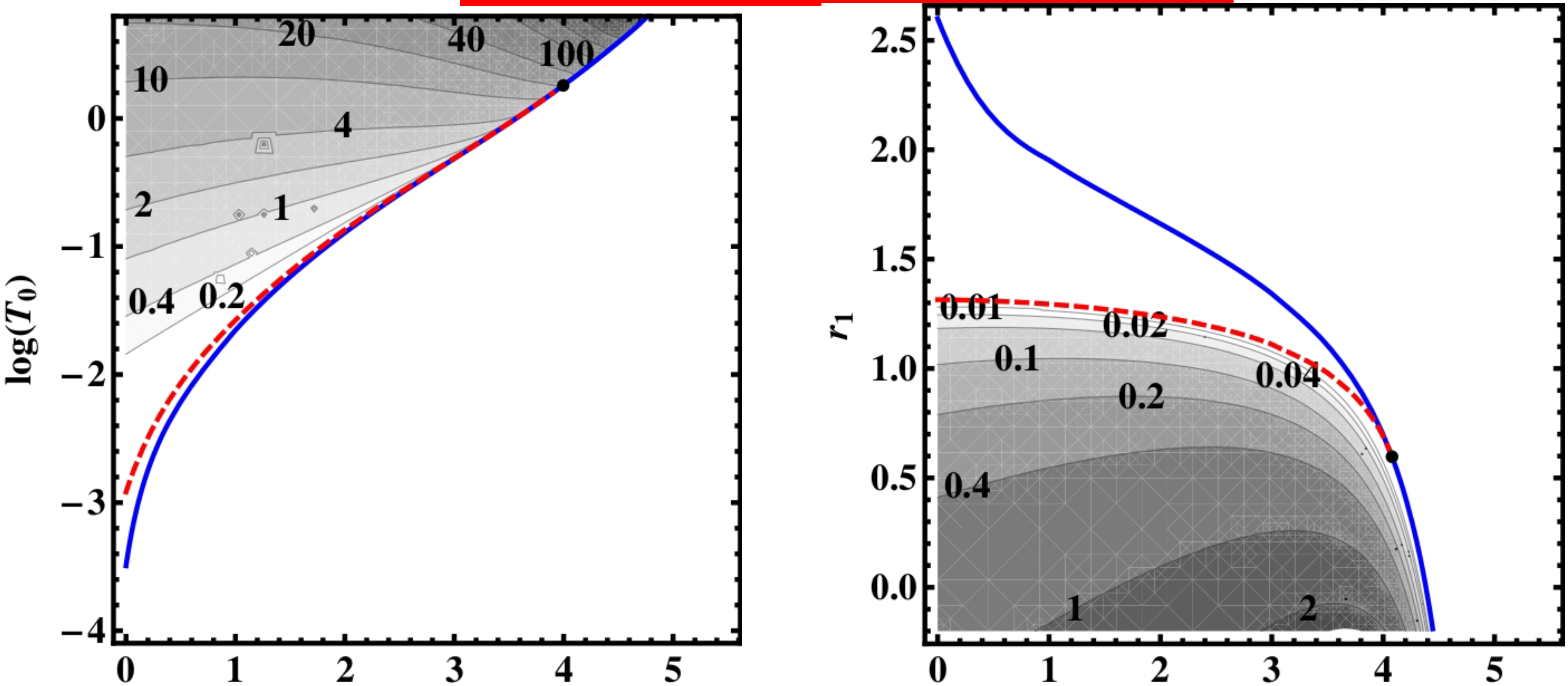

The UV behavior of the background solutions with good IR singularity for the scenario I (left) and parameter T_0 and scenario II (right) and parameter r_1.

The thick blue curve represents a change in the UV behavior, the red dashed curve has zero quark mass, and the contours give the quark mass. The black dot where the zero mass curve terminates lies at the critical value $x = x_c$. For scenario I (II) we have $x_c \simeq 3.9959$ ($x_c \simeq 4.0797$).

Numerical solutions: $T = 0$

$T \equiv 0$ backgrounds (color codes λ, A)

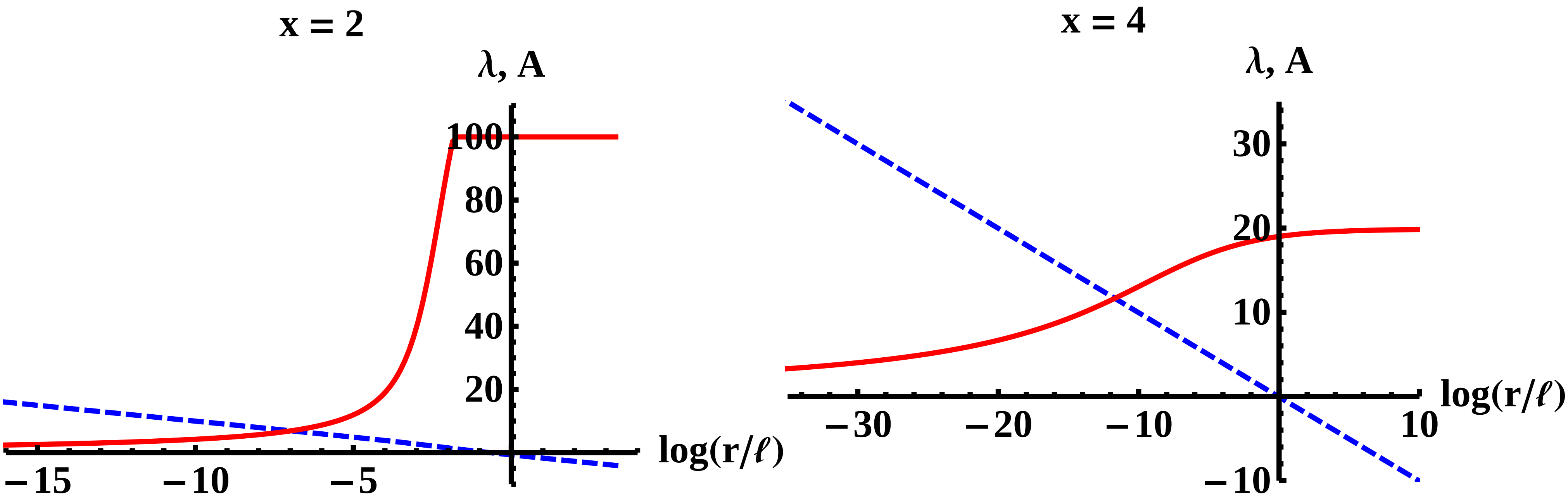

Numerical solutions: Massless with $x < x_c$

Massless backgrounds with $x < x_c \simeq 3.9959$ (λ, A, T)

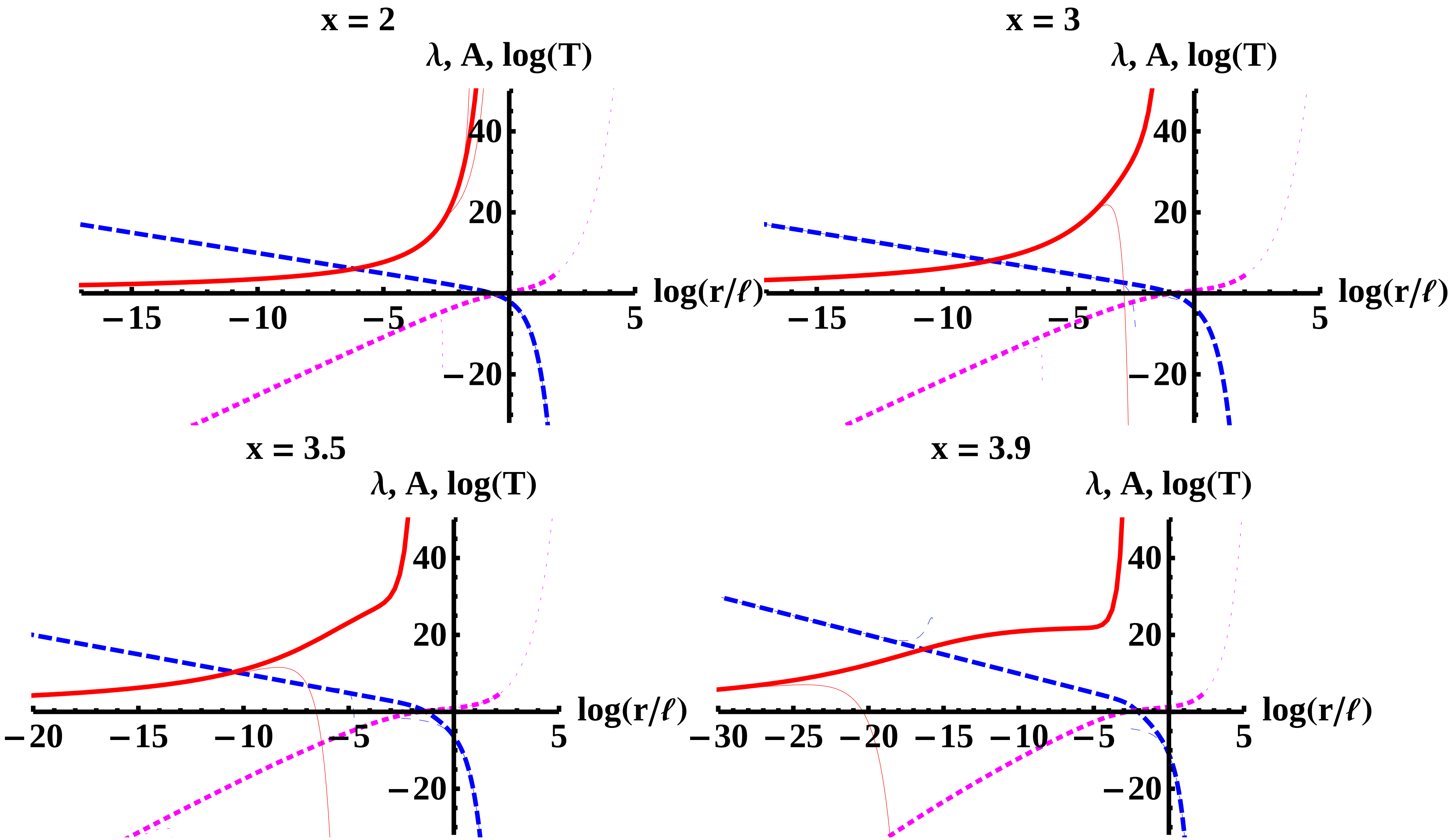

Massless backgrounds: beta functions $\beta = \frac{d\lambda}{dA}$, ($x_c \simeq 3.9959$)

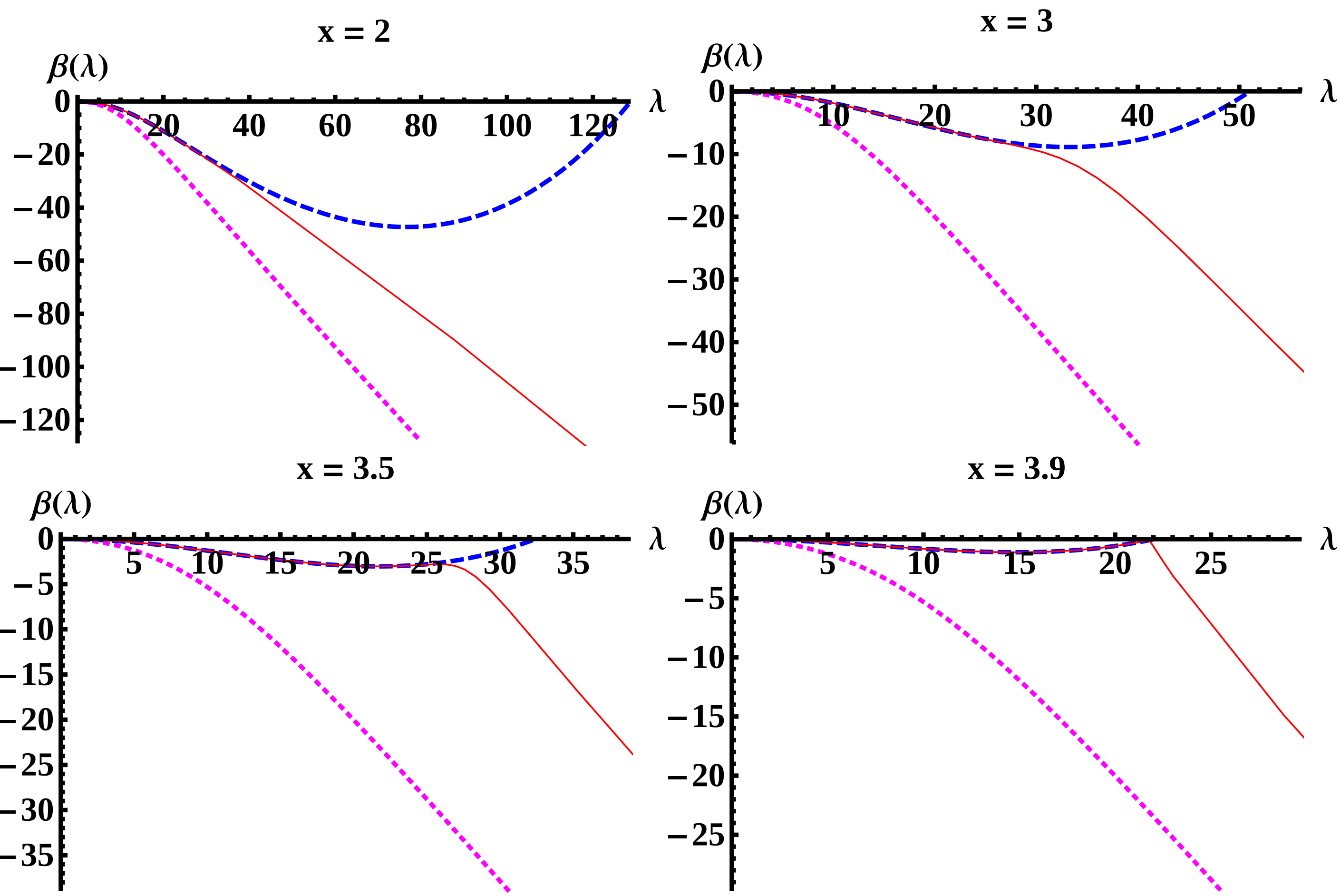

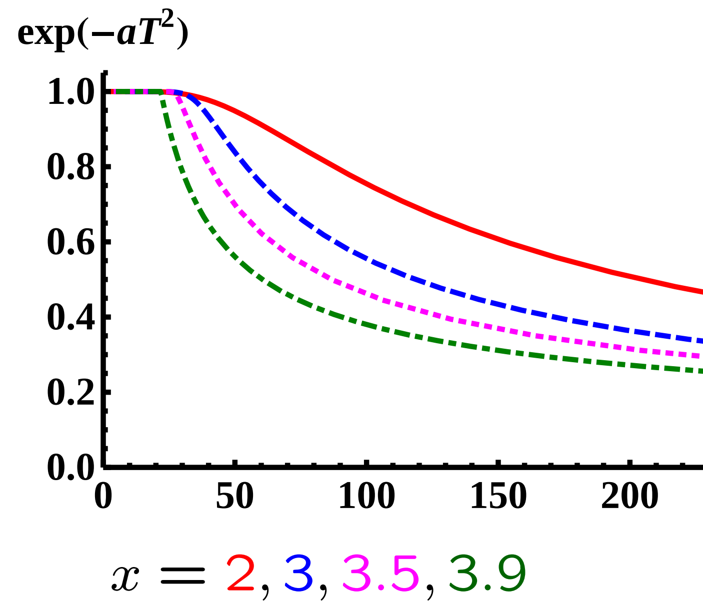

.

Massless backgrounds: gamma functions $\frac{\gamma}{T} = \frac{d \log T}{dA}$

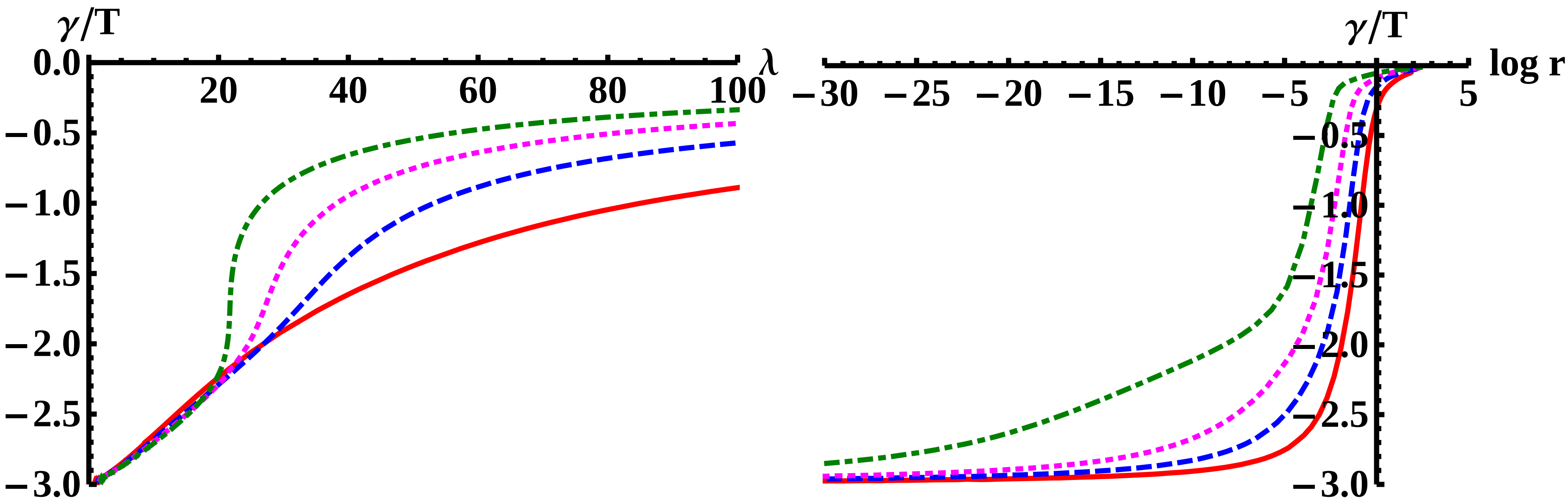

$x = 2, 3, 3.5, 3.9$

Matching to QCD: IR

• In the IR, the tachyon has to diverge $\Rightarrow$ the tachyon action $\propto e^{-T^2}$ becomes small

♠ $V_g(\lambda) \simeq \lambda^{\frac{4}{3}}\sqrt{\lambda}$ chosen as for Yang-Mills, so that a "good" IR singularity exists etc.

♠ $V_0(\lambda)$, $a(\lambda)$, and $h(\lambda)$ chosen to produce tachyon divergence: there are several possibilities.

♠ The phase structure is essentially independent of IR choices.

Choice I:

$$V_g(\lambda) = 12 + \frac{44}{9\pi^2}\lambda + \frac{4619}{3888\pi^4}\frac{\lambda^2}{(1+\lambda/(8\pi^2))^{2/3}}\sqrt{1+\log(1+\lambda/(8\pi^2))}$$

$$V_f(\lambda, T) = V_0(\lambda)e^{-a(\lambda)T^2}$$

$$V_0(\lambda) = \frac{12}{11} + \frac{4(33-2x)}{99\pi^2}\lambda + \frac{23473 - 2726x + 92x^2}{42768\pi^4}\lambda^2$$

$$a(\lambda) = \frac{3}{22}(11-x)$$

$$h(\lambda) = \frac{1}{\left(1 + \frac{115-16x}{288\pi^2}\lambda\right)^{4/3}}$$

For which in the IR

$$T(r) \sim T_0 \exp\left[\frac{81\ 3^{5/6}(115-16x)^{4/3}(11-x)}{812944\ 2^{1/6}}\frac{r}{R}\right] \quad , \quad r \to \infty$$

R is the IR scale of the solution. T_0 is the control parameter of the UV mass.

Choice II:

$$a(\lambda) = \frac{3}{22}(11-x)\frac{1+\frac{115-16x}{216\pi^2}\lambda+\frac{\lambda^2}{\lambda_0^2}}{(1+\lambda/\lambda_0)^{4/3}}$$

$$h(\lambda) = \frac{1}{(1+\lambda/\lambda_0)^{4/3}}$$

for which in the IR

$$T(r) \sim \frac{27\ 2^{3/4}3^{1/4}}{\sqrt{4619}}\sqrt{\frac{r-r_1}{R}} \quad , \quad r \to \infty$$

R is the IR scale of the solution. r_1 is the control parameter of the UV mass.

Comparison to previous "guesses"

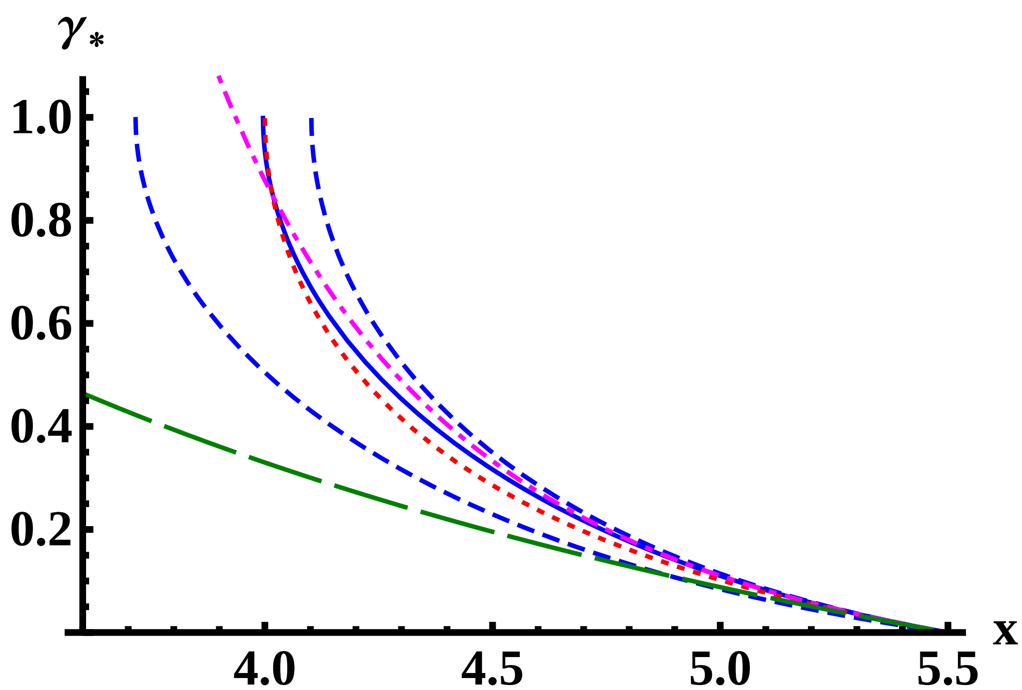

The anomalous dimension of the quark mass at the IR fixed point as a function of x within the conformal window in various approaches.

The solid blue curve is our result for the potential I.

The dashed blue lines show the maximal change as W_0 is varied from 0 (upper curve) to 24/11 (lower curve).

The dotted red curve is the result from a Dyson-Schwinger analysis, the dot-dashed magenta curve is the prediction of two-loop perturbative QCD, and the long-dashed green curve is based on an all-orders β-function.

Miransky scaling for the masses

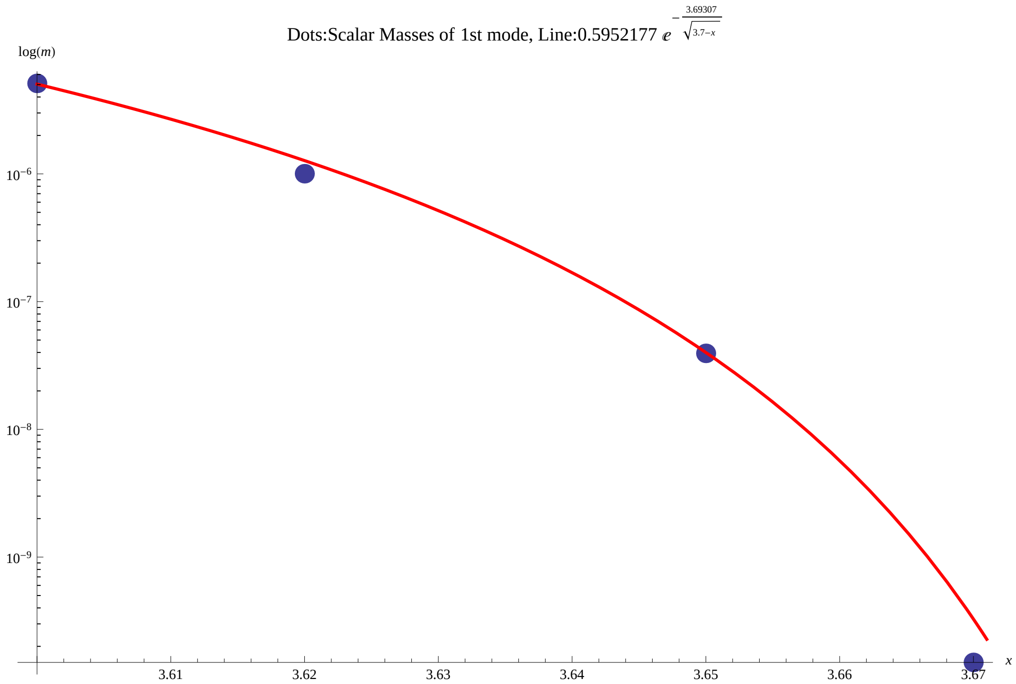

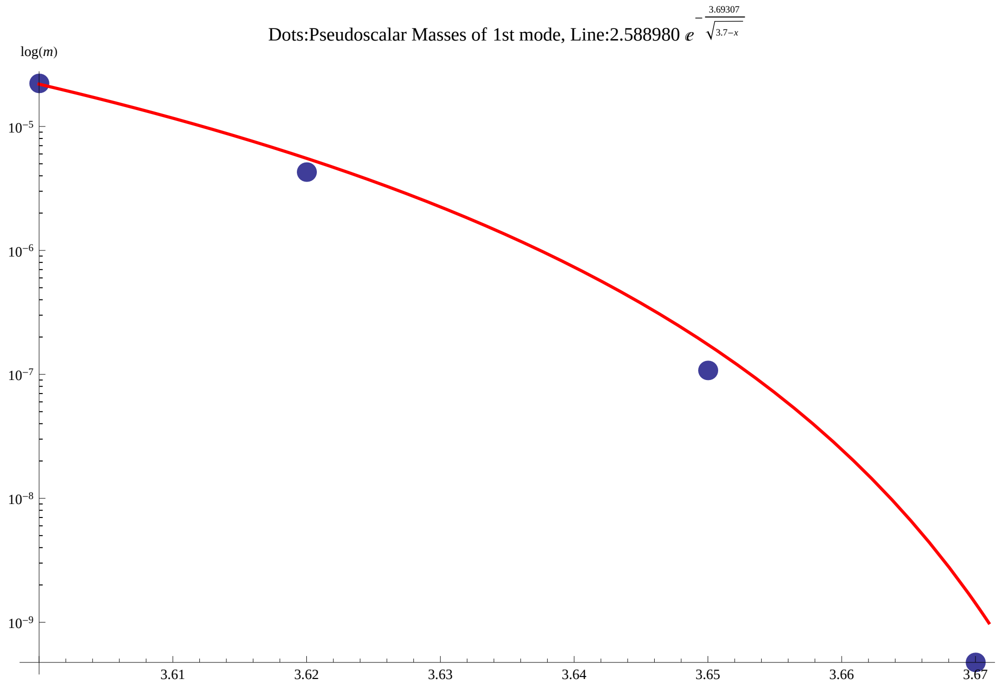

The plots depict the scalar and pseudoscalar masses of the first mode close to x_c fit to the Miransky exponential factor.

RETURN

The holographic models: flavor

- Fundamental quarks arise from $D4$-$\bar{D}4$ branes in 5-dimensions.

$$D4 - D4 \quad \text{strings} \quad \to \quad A_\mu^L \quad \leftrightarrow \quad J_\mu^L = \bar{\psi}_L \sigma_\mu \psi_L$$

$$\overline{D4} - \overline{D4} \quad \text{strings} \quad \to \quad A_\mu^R \quad \leftrightarrow \quad J_\mu^R = \bar{\psi}_R \bar{\sigma}_\mu \psi_R$$

$$D4 - \overline{D4} \quad \text{strings} \quad \to \quad T \quad \leftrightarrow \quad \bar{\psi}_L \psi_R$$

- For the vacuum structure only the tachyon is relevant.

- An action for the tachyon motivated by the Sen action has been advocated as the proper dynamics of the chiral condensate, giving in general all the expected features of χSB.

Casero+Kiritsis+Paredes

$$\mathcal{S}_{\rm TDBI} = -N_f N_c M^3 \int d^5x \; V_f(T) \; e^{-\phi} \sqrt{-\det(g_{ab} + \partial_a T \partial_b T)}$$

- It has been tested in a 6d asymptotically-AdS confining background (with constant dilaton) due to Kuperstein+Sonneschein.

Iatrakis+Kiritsis+Paredes

It was shown to have the following properties:

- Confining asymptotics of the geometry trigger chiral symmetry breaking.

- A Gell-Mann-Oakes-Renner relation is generically satisfied.

- The Sen DBI tachyon action with $V \sim e^{-T^2}$ asymptotics induces linear Regge trajectories for mesons.

- The Wess-Zumino (WZ) terms of the tachyon action, computed in string theory, produce the appropriate flavor anomalies, include the axial $U(1)$ anomaly and η'-mixing, and implement a holographic version of the Coleman-Witten theorem.

- The dynamics determines the chiral condensate uniquely a s function of the bare quark mass.

- The mass of the ρ-meson grows with increasing quark mass.

- By adjusting the same parameters as in QCD ($\Lambda_{\rm QCD}$, m_{ud}) a good fit can be obtained of the light meson masses.

The chiral vacuum structure

• We take the potential to be the flat space one

$$V = V_0 \, e^{-T^2}$$

with a maximum at $T = 0$ and a minimum at $T = \infty$.

• Near the boundary $z = 0$, the solution can be expanded in terms of two integration constants as:

$$\tau = c_1 z + \frac{\pi}{6} c_1^3 z^3 \log z + c_3 z^3 + \mathcal{O}(z^5)$$

• c_1, c_3 are related to the quark mass and condensate.

• At the tip of the cigar, the generic behavior of solutions is

$$\tau \sim constant_1 + constant_2 \sqrt{z - z_\Lambda}$$

• With special tuned condition there is a one-parameter family of diverging solutions in the IR depending on a single parameter:

$$\tau = \frac{C}{(z_\Lambda - z)^{\frac{3}{20}}} - \frac{13}{6\pi C}(z_\Lambda - z)^{\frac{3}{20}} + \ldots$$

• This is the correct "regularity condition" in the IR as τ is allowed to diverge only at the tip.

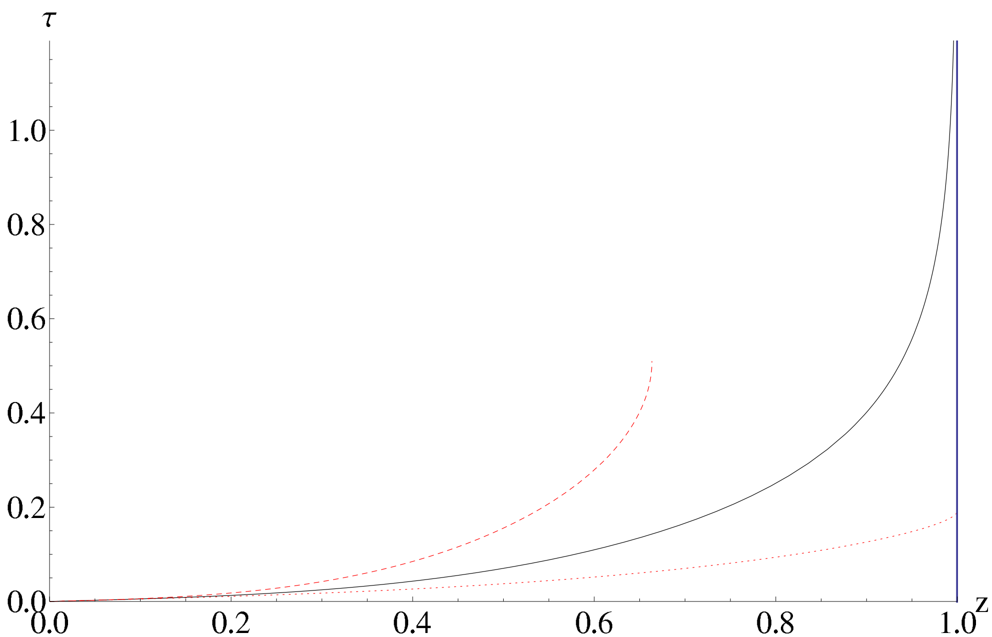

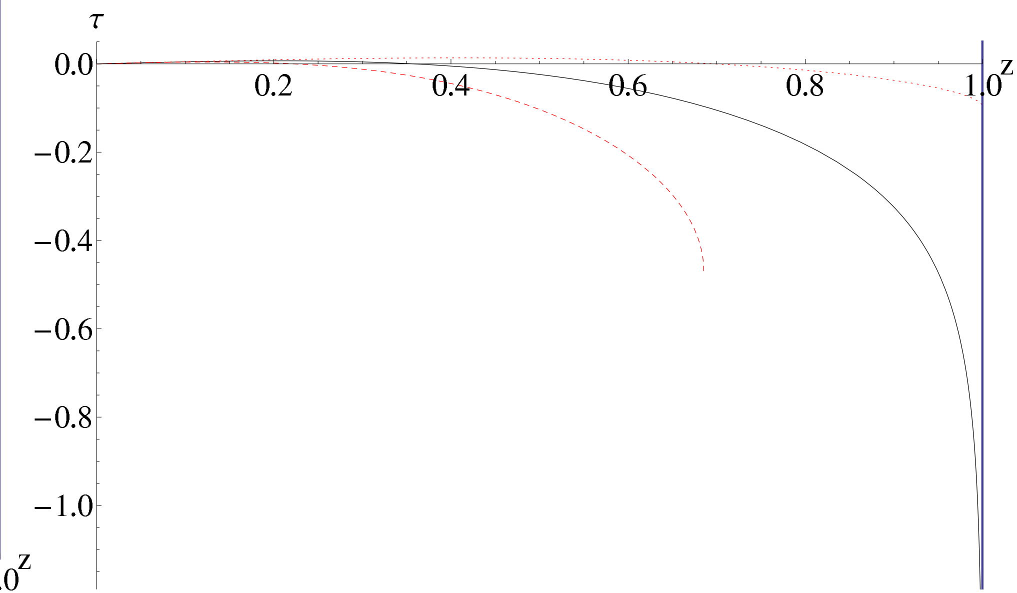

All the graphs are plotted using $z_\Lambda = 1$, $\mu^2 = \pi$ and $c_1 = 0.05$. The tip of the cigar is at $z = z_\Lambda = 1$. On the left, the solid black line represents a solution with $c_3 \approx 0.3579$ for which τ diverges at z_Λ. The red dashed line has a too large c_3 ($c_3 = 1$) - such that there is a singularity at $z = z_s$ where $\partial_z \tau$ diverges while τ stays finite. This is unacceptable since the solution stops at $z = z_s$ where the energy density of the flavor branes diverges. The red dotted line corresponds to $c_3 = 0.1$; this kind of solution is discarded because the tachyon stays finite everywhere. The plot in the right is done with the same conventions but with negative values of $c_3 = -0.1, -0.3893, -1$. For $c_3 \approx -0.3893$ there is a solution of the differential equation such that τ diverges to $-\infty$. This solution is unstable.

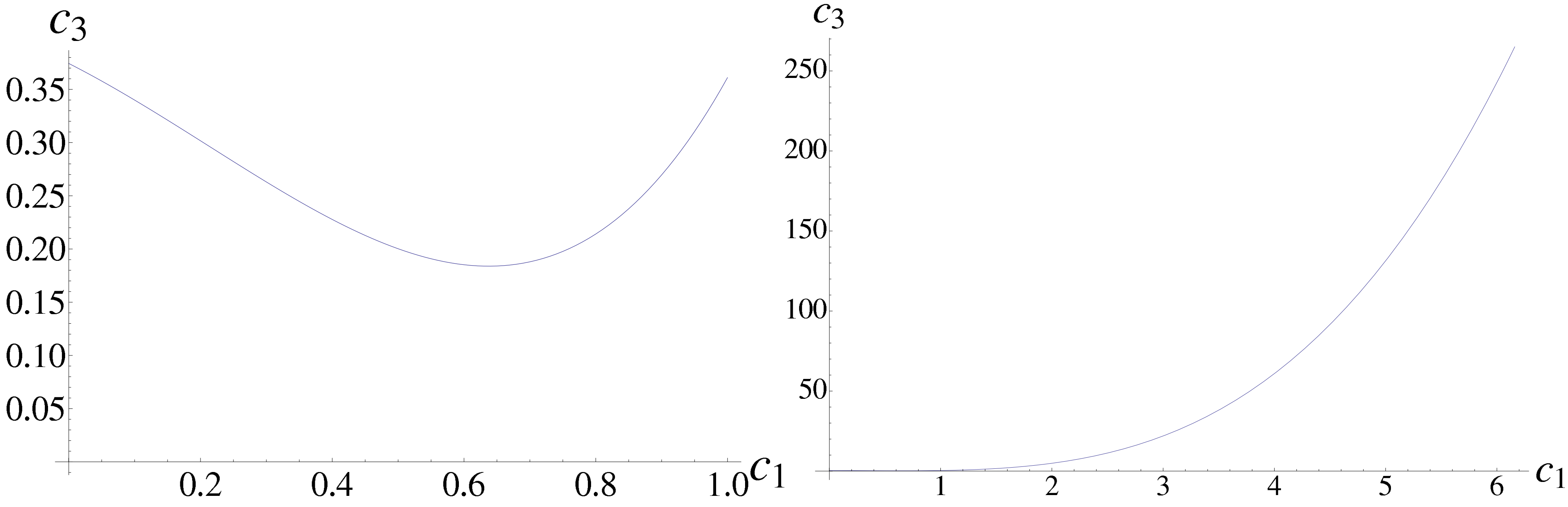

- Chiral symmetry breaking is manifest.

Chiral restauration at deconfinement

- In the deconfined phase, the bulk metric is that of a bh.
- The branes now are allowed to enter the horizon without recombining.
- To avoid intermediate singularities of the solution the boundary conditions must be tuned so that tachyon is finite at the horizon.
- Near the horizon the correct solution behaves as a one-parameter family

$$\tau = c_T - \frac{3c_T}{5z_T}(z_T - z) - \frac{9c_T}{200z_T}(8 + \mu^2 {c_T}^2)(z_T - z)^2 + \ldots$$

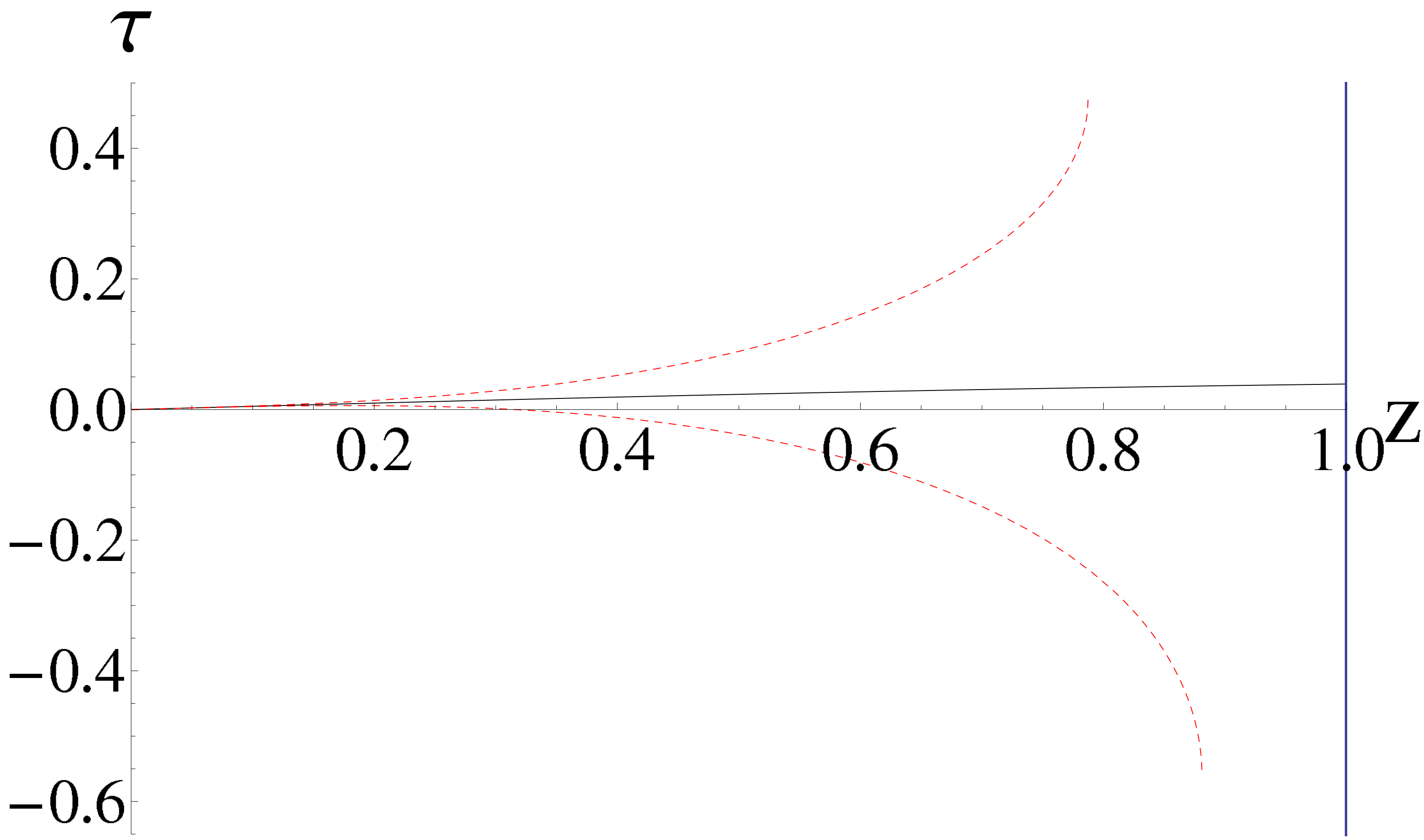

Plots corresponding to the deconfined phase. We have taken $c_1 = 0.05$. The solid line displays the physical solution $c_3 = -0.0143$ whereas the dashed lines ($c_3 = -0.5$ and $c_3 = 0.5$) are unphysical and end with a behavior of the type $\tau = k_1 - k_2\sqrt{z_s - z}$.

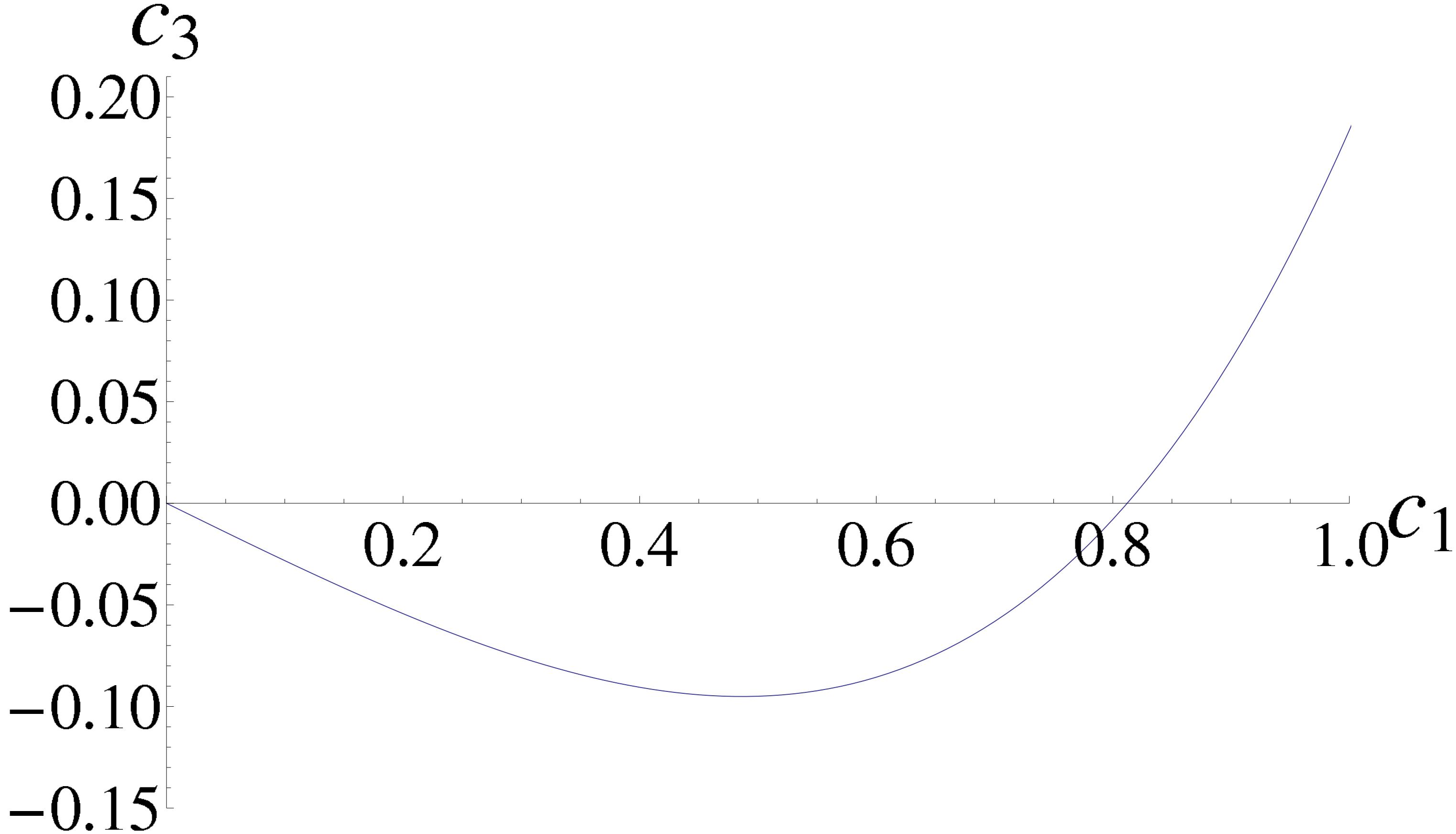

These plots give the values of c_3 determined numerically by demanding the correct IR behavior of the solution, as a function of c_1.

Jump of the condensate at the phase transition

- From holographic renormalization we obtain

$$\langle \bar{q}q \rangle = \frac{1}{\beta}(2\pi\alpha'\mathcal{K}R^3\lambda)\left(-4c_3 + \left(\frac{m_q}{\beta}\right)^3 \mu^2(1+\alpha)\right) \quad , \quad m_q = \beta\ c_1$$

- We calculate the jump at the phase transition that is scheme independent for a fixed quark mass.

$$\Delta\langle \bar{q}q \rangle \equiv \langle \bar{q}q \rangle_{conf} - \langle \bar{q}q \rangle_{deconf} = -4\frac{1}{\beta}(2\pi\alpha'\mathcal{K}R^3\lambda)\Delta c_3$$

- This is equivalent to Δc_3

• We plot it as a function of the quark mass.

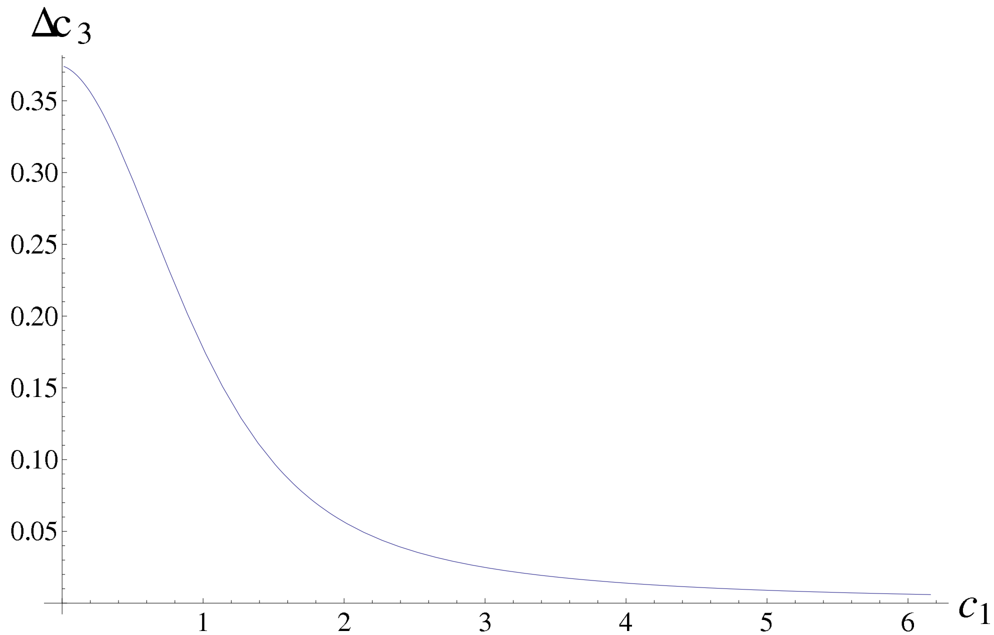

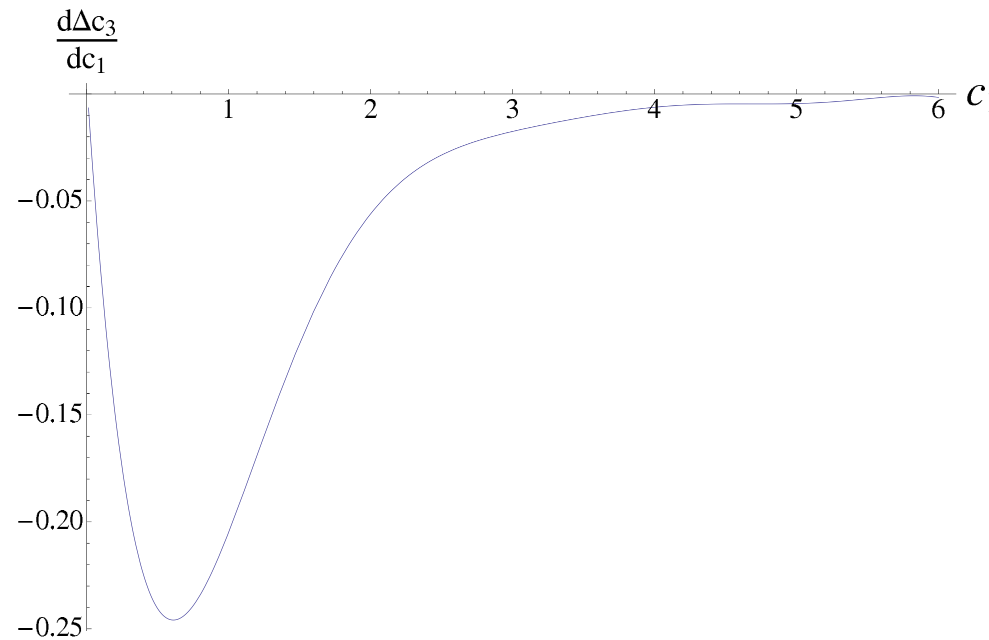

The finite jump of the quark condensate and its derivative with respect to c_1 when the confinement-deconfinement transition takes place. The important features appear when $m_q \sim \Lambda_{QCD}$

Meson spectra

For the vectors

$$z_\Lambda m_V^{(1)} = 1.45 + 0.718 c_1 , \quad z_\Lambda m_V^{(2)} = 2.64 + 0.594 c_1 , \quad z_\Lambda m_V^{(3)} = 3.45 + 0.581 c_1 ,$$
$$z_\Lambda m_V^{(4)} = 4.13 + 0.578 c_1 , \quad z_\Lambda m_V^{(5)} = 4.72 + 0.577 c_1 , \quad z_\Lambda m_V^{(6)} = 5.25 + 0.576 c_1 .$$

For the axial vectors:

$$z_\Lambda m_A^{(1)} \approx 2.05 + 1.46 c_1 , \quad z_\Lambda m_A^{(2)} \approx 3.47 + 1.24 c_1 , \quad z_\Lambda m_A^{(3)} \approx 4.54 + 1.17 c_1 ,$$
$$z_\Lambda m_A^{(4)} \approx 5.44 + 1.13 c_1 , \quad z_\Lambda m_A^{(5)} \approx 6.23 + 1.11 c_1 , \quad z_\Lambda m_A^{(6)} \approx 6.95 + 1.10 c_1 .$$

For the pseudoscalars:

$$z_\Lambda m_P^{(1)} \approx \sqrt{3.53 c_1^2 + 6.33 c_1} , \quad z_\Lambda m_P^{(2)} \approx 2.91 + 1.40 c_1 , \quad z_\Lambda m_P^{(3)} \approx 4.07 + 1.27 c_1 ,$$
$$z_\Lambda m_P^{(4)} \approx 5.04 + 1.21 c_1 , \quad z_\Lambda m_P^{(5)} \approx 5.87 + 1.17 c_1 , \quad z_\Lambda m_P^{(6)} \approx 6.62 + 1.15 c_1 .$$

For the scalars:

$$z_\Lambda m_S^{(1)} = 2.47 + 0.683 c_1 , \quad z_\Lambda m_S^{(2)} = 3.73 + 0.488 c_1 , \quad z_\Lambda m_S^{(3)} = 4.41 + 0.507 c_1 ,$$
$$z_\Lambda m_S^{(4)} = 4.99 + 0.519 c_1 , \quad z_\Lambda m_S^{(5)} = 5.50 + 0.536 c_1 , \quad z_\Lambda m_S^{(6)} = 5.98 + 0.543 c_1 .$$

- Valid up to $c_1 \sim 1$.
- In qualitative agreement with lattice results
  Laerman+Schmidt., Del Debbio+Lucini+Patela+Pica, Bali+Bursa

Mass dependence of f_π

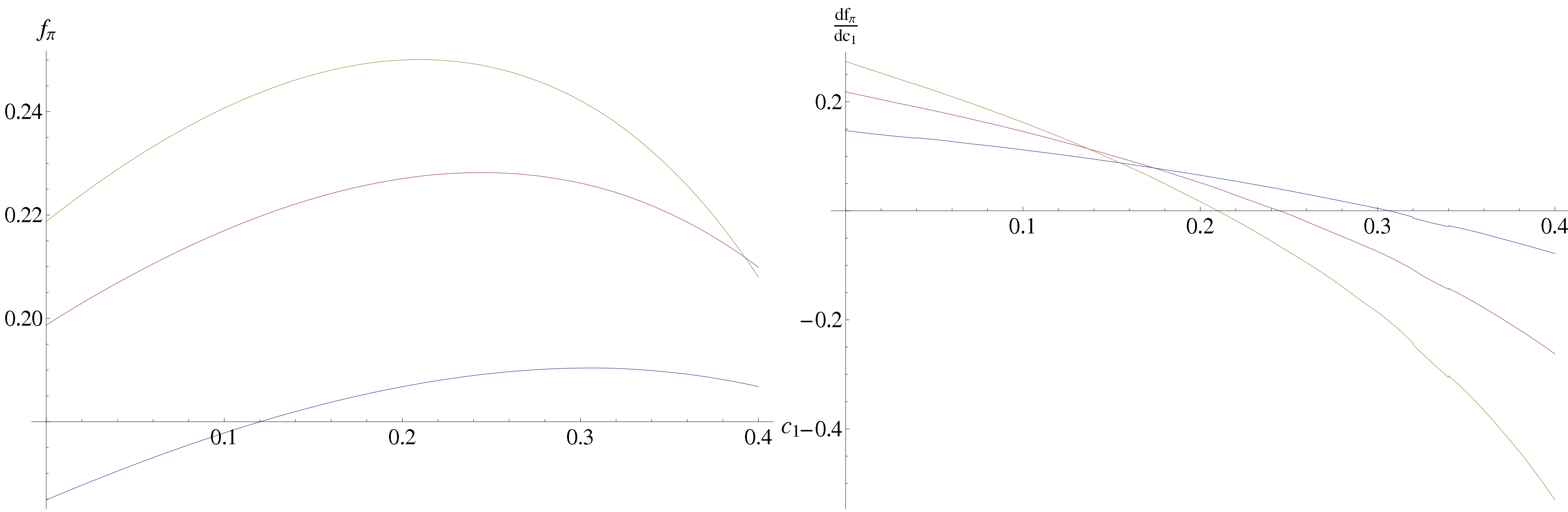

The pion decay constant and its derivative as a function of c_1 - the quark mass. The different lines correspond to different values of k. From bottom to top (on the right plot, from bottom to top in the vertical axis) $k = \frac{12}{\pi^2}, \frac{24}{\pi^2}, \frac{36}{\pi^2}$. The pion decay constant comes in units of z_Λ^{-1}.

Linear Regge Trajectories

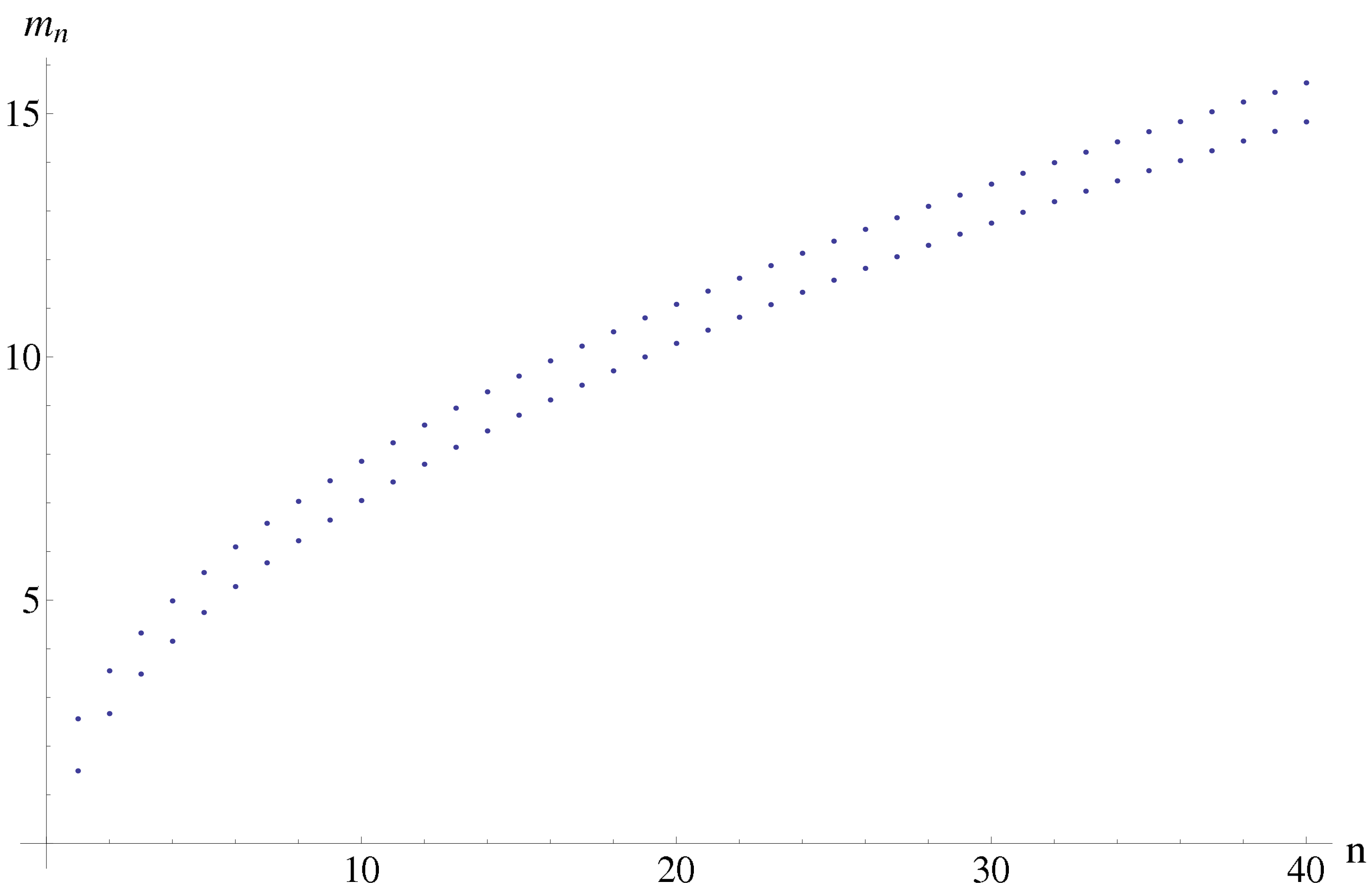

Results corresponding to the forty lightest vector states with $c_1 = 0.05$ and $c_1 = 1.5$.

Walking

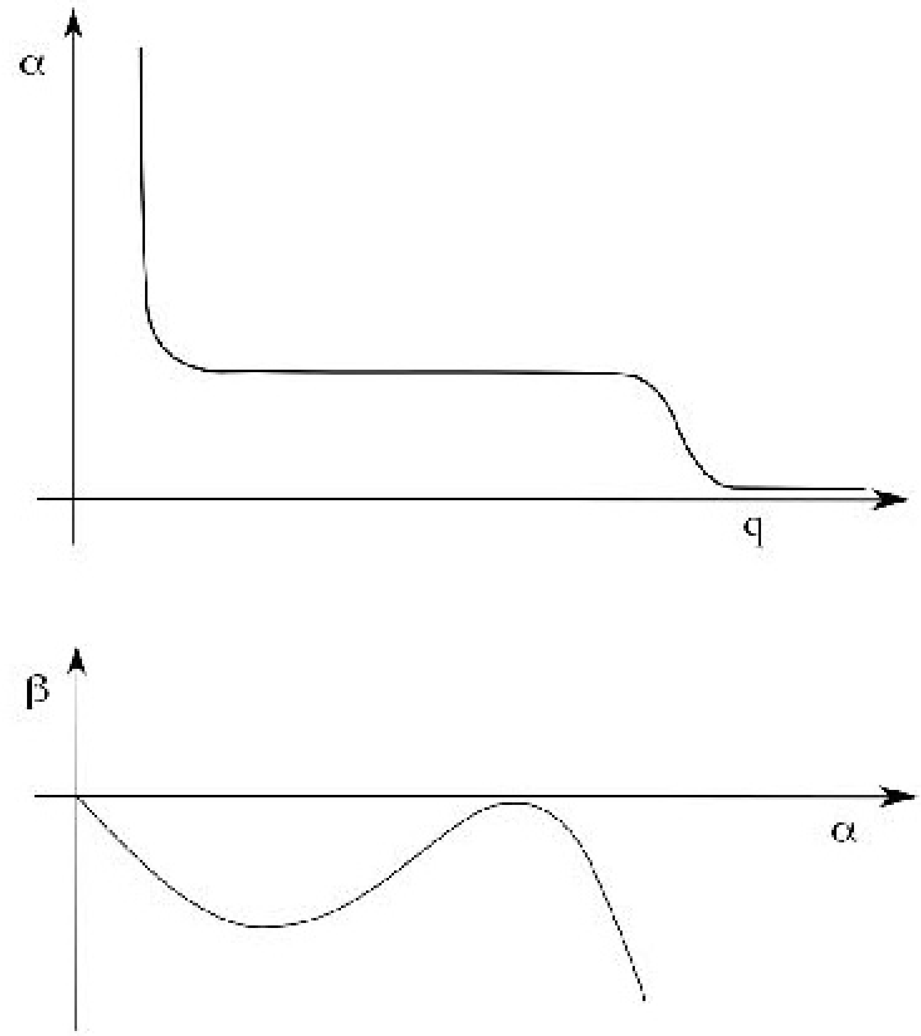

RETURN

The phase diagram

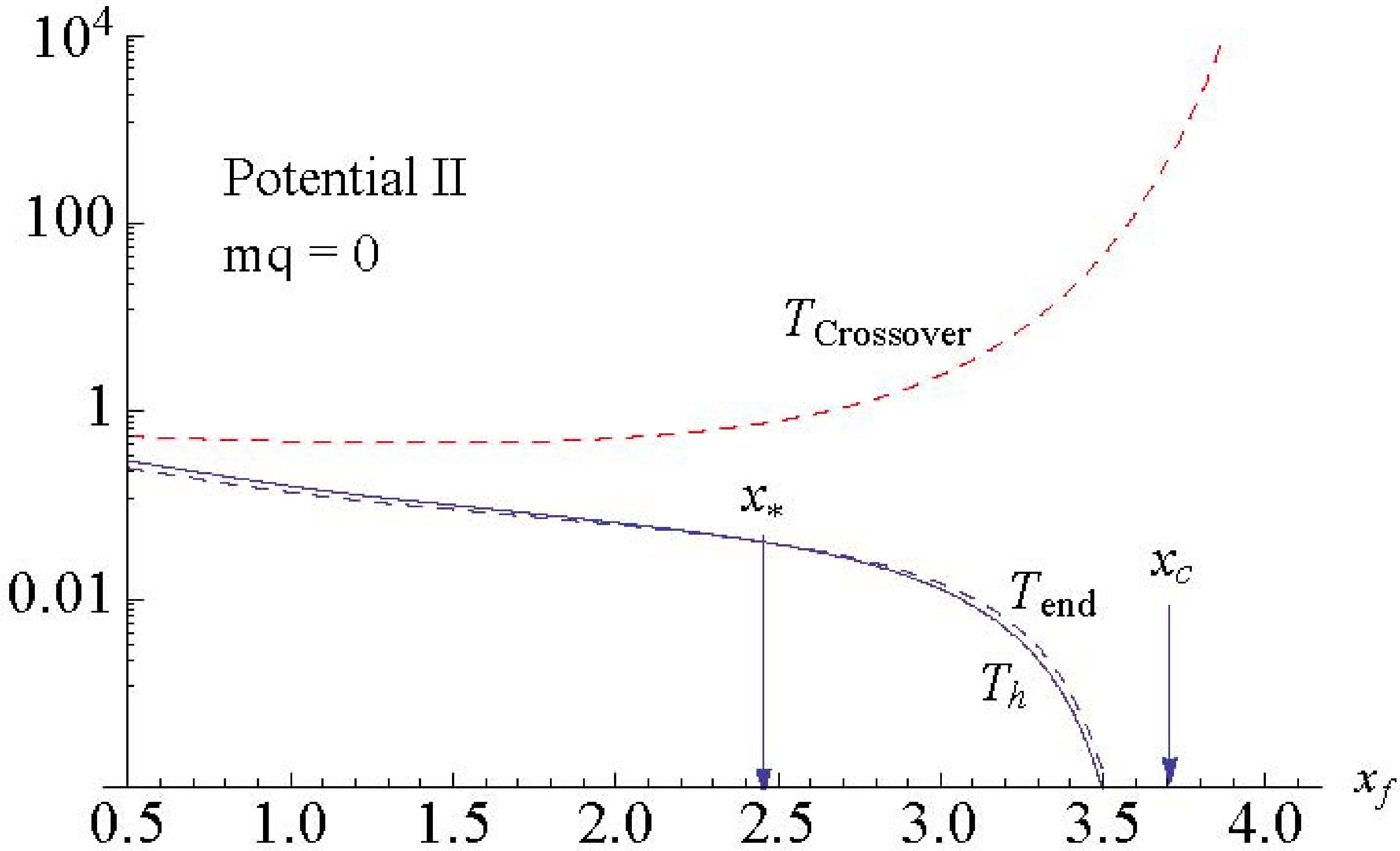

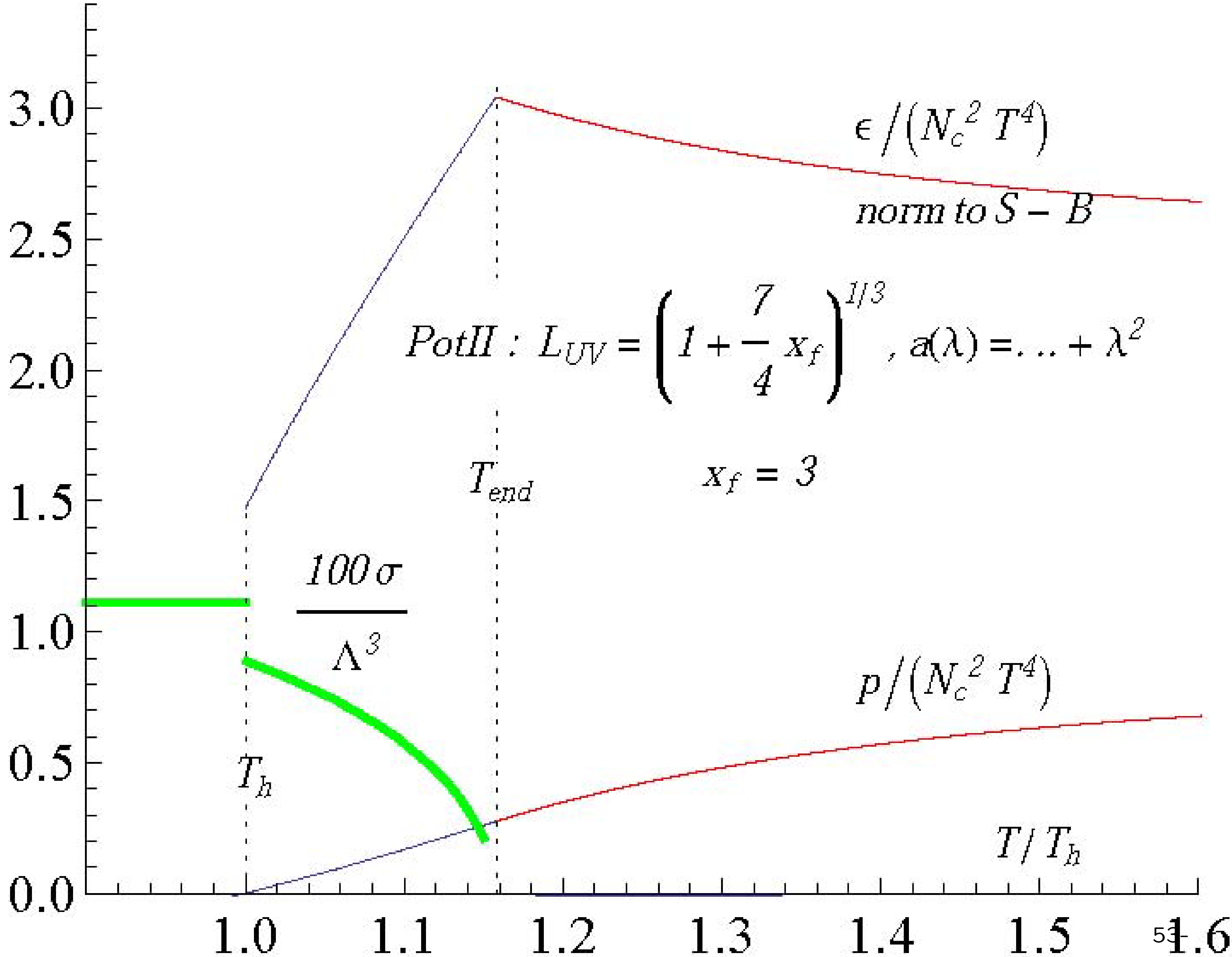

$\epsilon/(N_c^2 T^4)$
norm to S − B
$PotII : L_{UV} = \left(1 + \frac{7}{4} x_f\right)^{1/3}, a(\lambda) = \ldots + \lambda^2$
T_{end}
$x_f = 3$
$\frac{100\,\sigma}{\Lambda^3}$
$p/(N_c^2 T^4)$
T_h
T/T_h
0.0
0.5
1.0
1.5
2.0
2.5
3.0
1.0
1.1
1.2
1.3
1.4
1.5
1.6

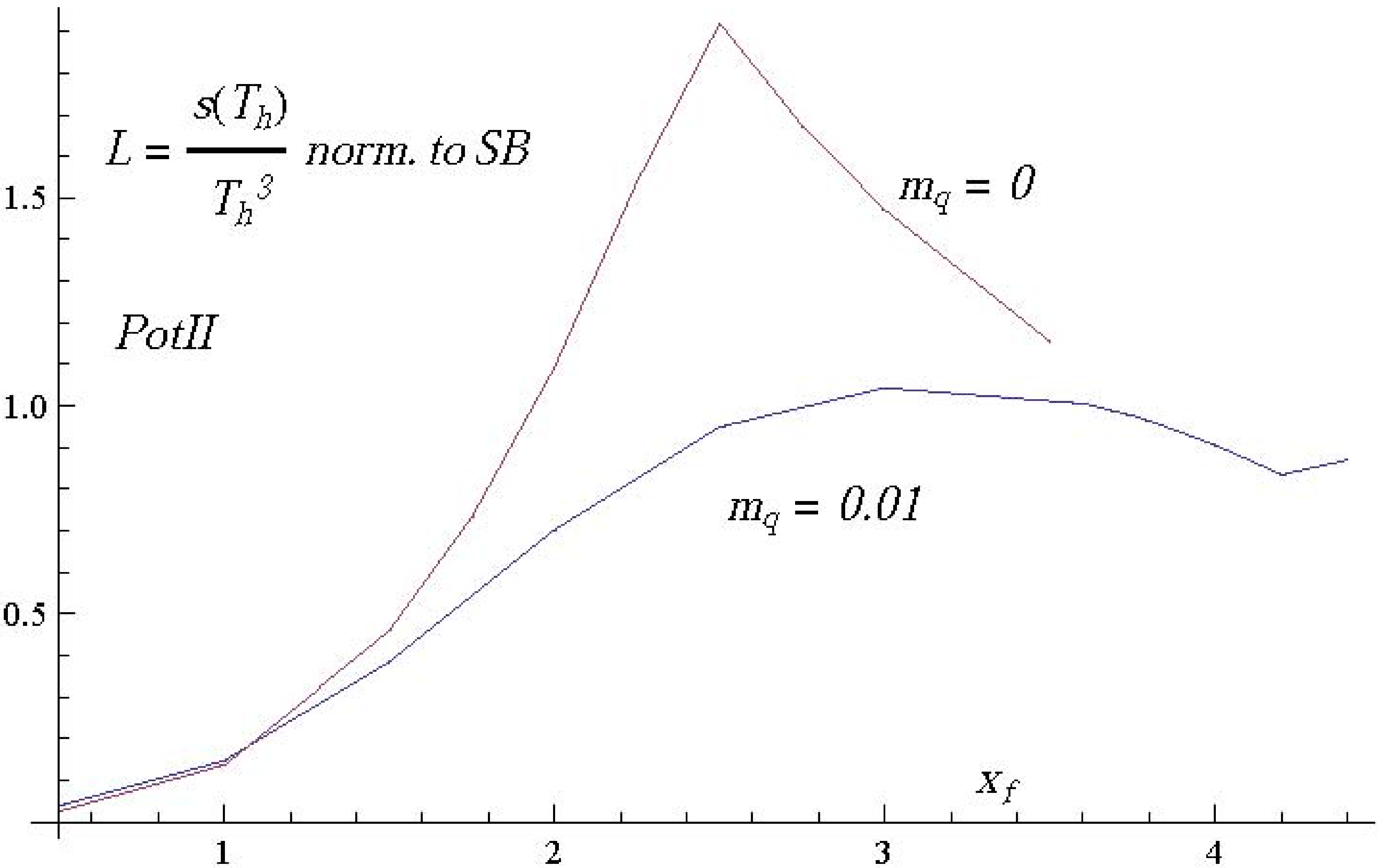
$L = \frac{s(T_h)}{T_h^{\,3}}$ norm. to SB
PotII
$m_q = 0$
$m_q = 0.01$
1.5
1.0
0.5
1
2
3
4
x_f

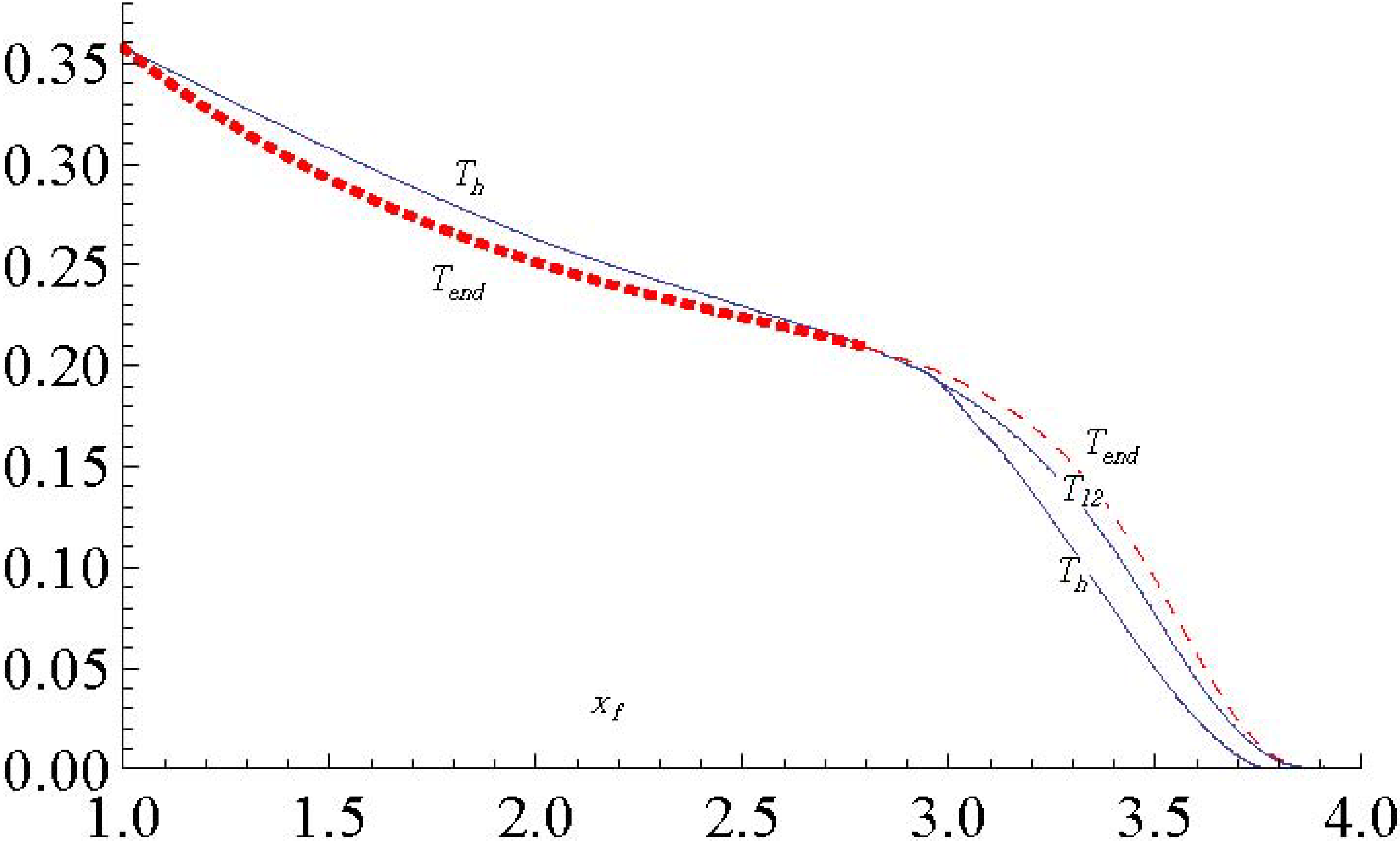

0.35
0.30
0.25
0.20
0.15
0.10
0.05
0.00
1.0
1.5
2.0
2.5
3.0
3.5
4.0
T_h
T_{end}
T_{end}
T_{12}
T_h
x_f

The improved Sen tachyon action

• The Sen action is conjectured for unstable branes and $D\bar{D}$ pairs in flat space. It passes several constraints on its dynamics.

• There are background independent arguments that $V_f \to 0$ when D-branes annihilate.

Sen

• The IhQCD background for glue, becomes flat in the string frame in the IR. The dilaton runs however (quadratically).

• The Sen action is expected to have open string corrections: these are not expected to change it basic asymptotics: $V_f \to 0$.

• The $\sqrt{|DT|^2}$ at large T is subleading and does not affect qualitatively the dynamics.

RETURN

The effective potential

For solutions $T = T_* = constant$ the relevant non-linear action simplifies

$$\mathcal{S} = M^3 N_c^2 \int d^5x \sqrt{g} \left[R - \frac{4}{3} \frac{(\partial\lambda)^2}{\lambda^2} + V_g(\lambda) - x V_f(\lambda, T) \right]$$

$$V_f(\lambda, T) = V_0(\lambda)\; e^{-a(\lambda) T_*^2}$$

• Minimizing for T_* we obtain $T_* = 0$ and $T_* = \infty$. The effective potential for λ is

♠ $T_* = 0$, $V_{eff} = V_g(\lambda) - x V_0(\lambda)$ with a IR fixed point at $\lambda = \lambda_*(x_f)$.

♠ $T_* = \infty$, $V_{eff} = V_g(\lambda)$ with no fixed points.

• From that point on, according to holography rules, we should find regular solutions for the metric, T and λ, that start with their sources in the UV (UV 't Hooft coupling and quark mass) and compare their free energies.

Characterizing IR asymptotics

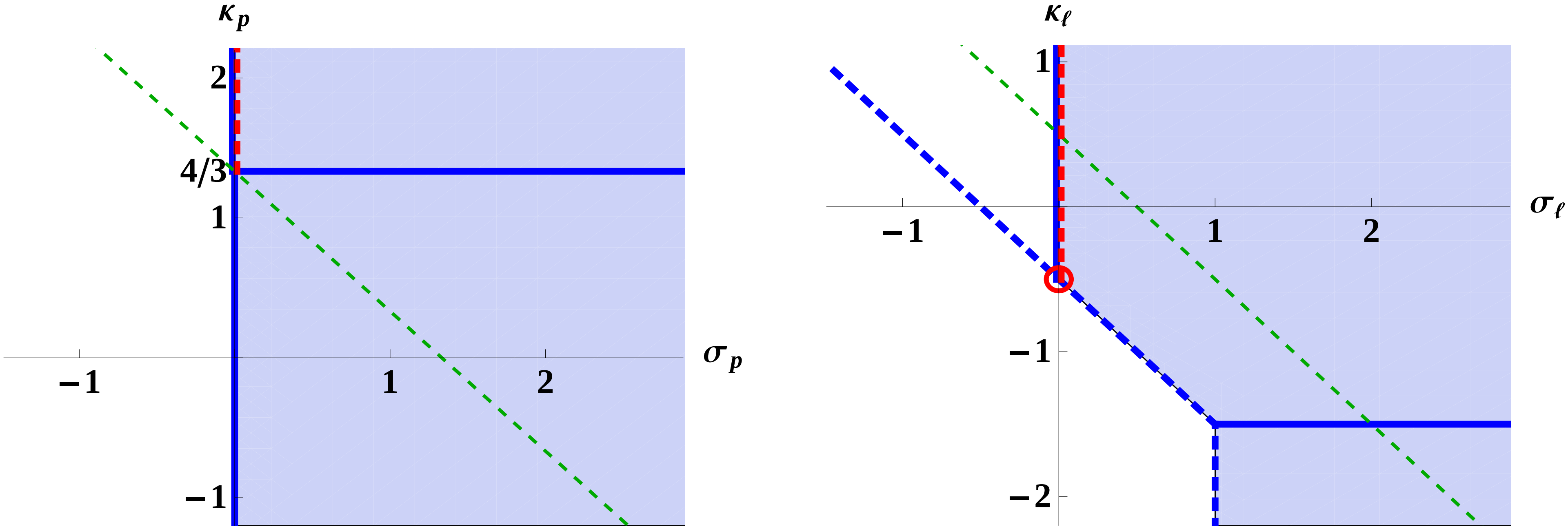

Map of the acceptable IR asymptotics of the functions $\kappa(\lambda) \sim \lambda^{-\kappa_p}(\log\lambda)^{-\kappa_\ell}$ and $a(\lambda) \sim \lambda^{\sigma_p}(\log\lambda)^{\sigma_\ell}$. Left: qualitatively different regions of tachyon asymptotics as a function of the parameters κ_p and a_p characterizing the power-law asymptotics of the functions. Right: regions of tachyon asymptotics at the critical point $\kappa_p = 4/3$, $a_p = 0$ as a function of the parameters κ_ℓ and a_ℓ characterizing the logarithmic corrections to the functions. In each plot, the shaded regions have acceptable IR behavior, and the thick blue lines denote changes in the qualitative IR behavior of the tachyon background. On the solid blue lines good asymptotics can be found, whereas on the dashed lines such asymptotics is absent. The thin dashed green line shows the critical behavior where the BF bound is saturated as $x \to 0$. Potentials above this line are guaranteed to have broken chiral symmetry at small x.

Finally, on the red dashed lines the asymptotic meson mass trajectories are linear with subleading logarithmic corrections. The red circle shows the single choice of parameters where the logarithmic corrections are absent.

Spectra

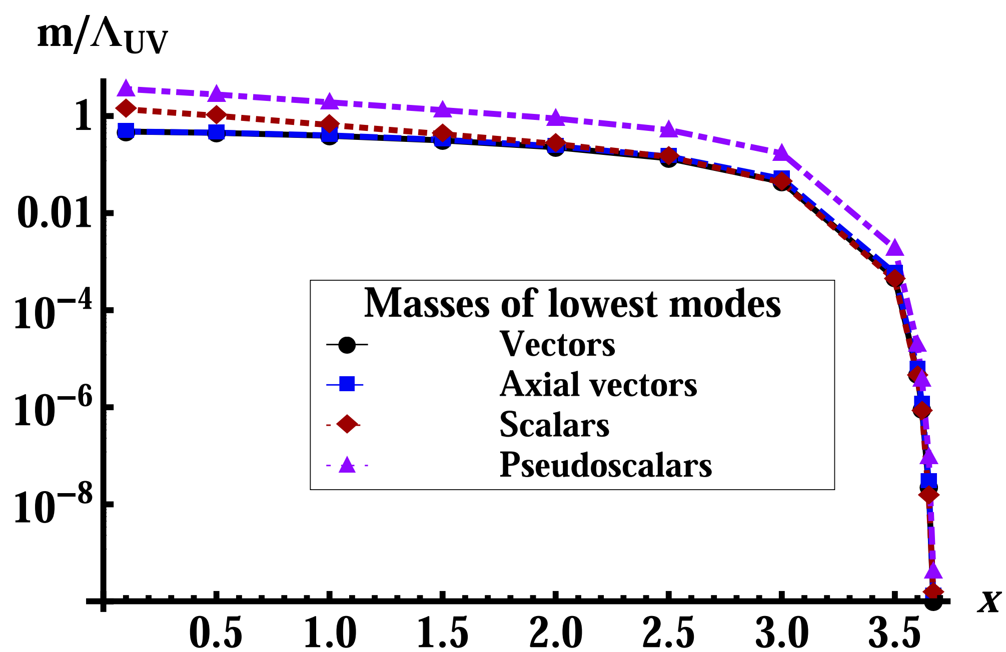

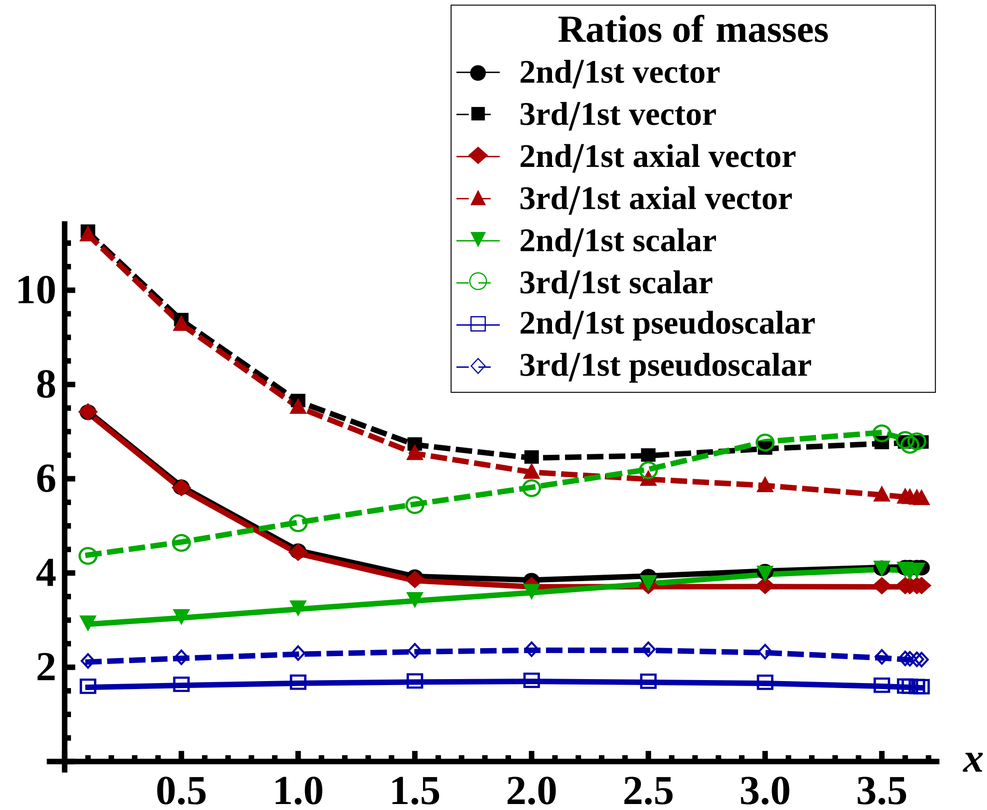

Non-singlet meson spectra in the potential II class with Stefan-Boltzmann (SB) normalization for W_0, with $x_c \simeq 3.7001$. Left: the lowest non-zero masses of all four towers of mesons, as a function of x, in units of $\Lambda_{\rm UV}$, below the conformal window. Right, the ratios of masses of up to the fourth massive states in the same theory as a function of x.

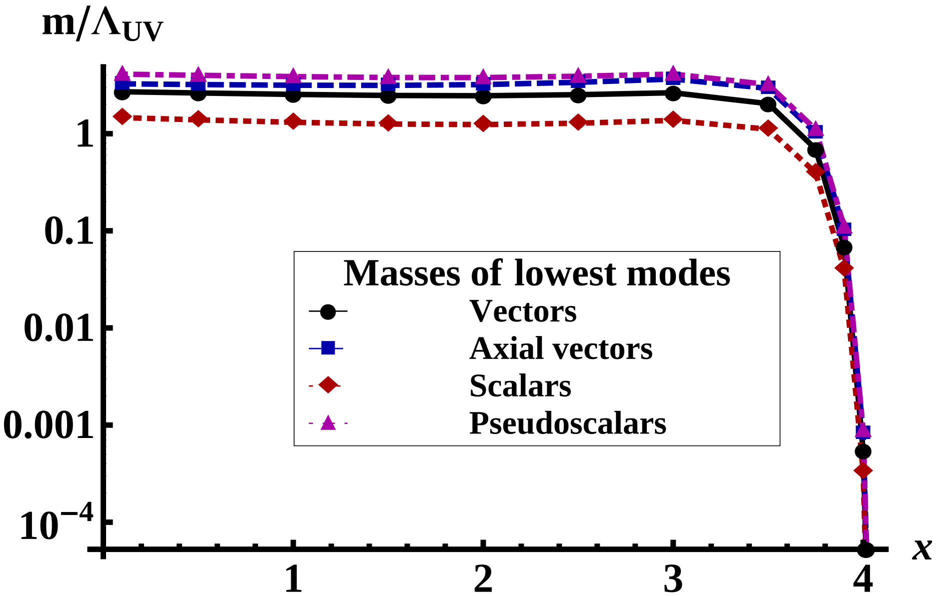

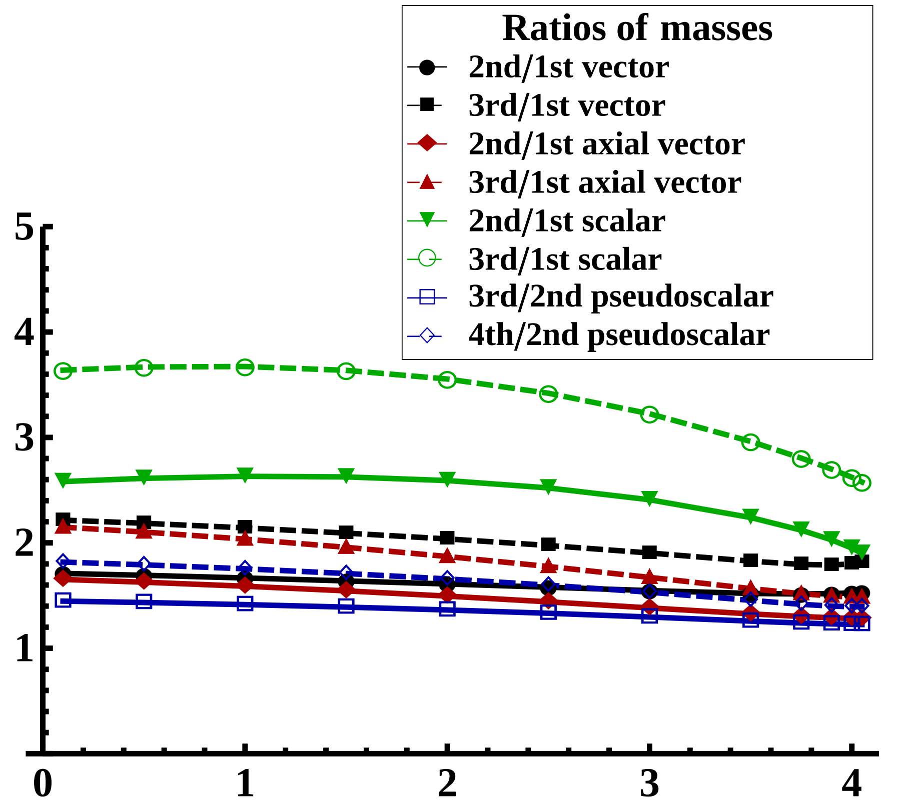

Non-singlet meson spectra in the potential I class ($W_0 = \frac{3}{11}$), with $x_c \simeq 4.0830$. Left: the lowest non-zero masses of all four towers of mesons, as a function of x, in units of $\Lambda_{\rm UV}$, below the conformal window. Right, the ratios of masses of up to the fourth massive states in the same theory as a function of x.

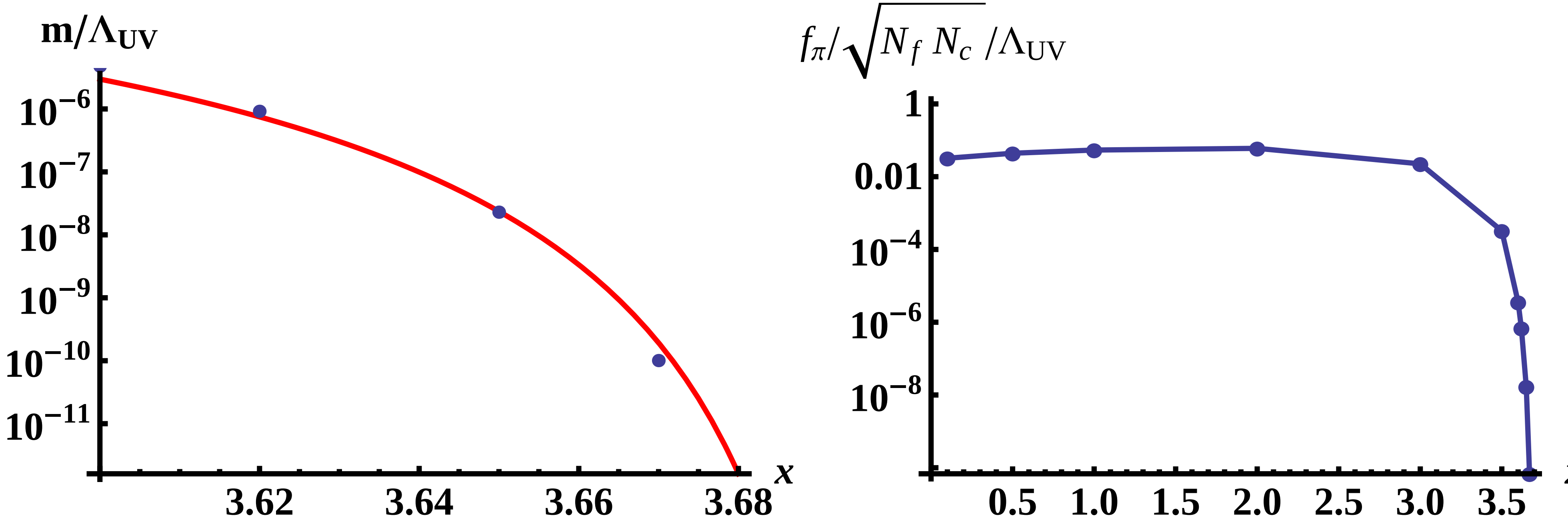

Potential II with SB normalization for W_0. Left: A fit of the ρ mass to the Miransky scaling factor, showing that it displays Miransky scaling in the walking region. Right, f_π as a function of x in units of $\Lambda_{\rm UV}$. It vanishes near x_c following again Miransky scaling.

Finite small mass

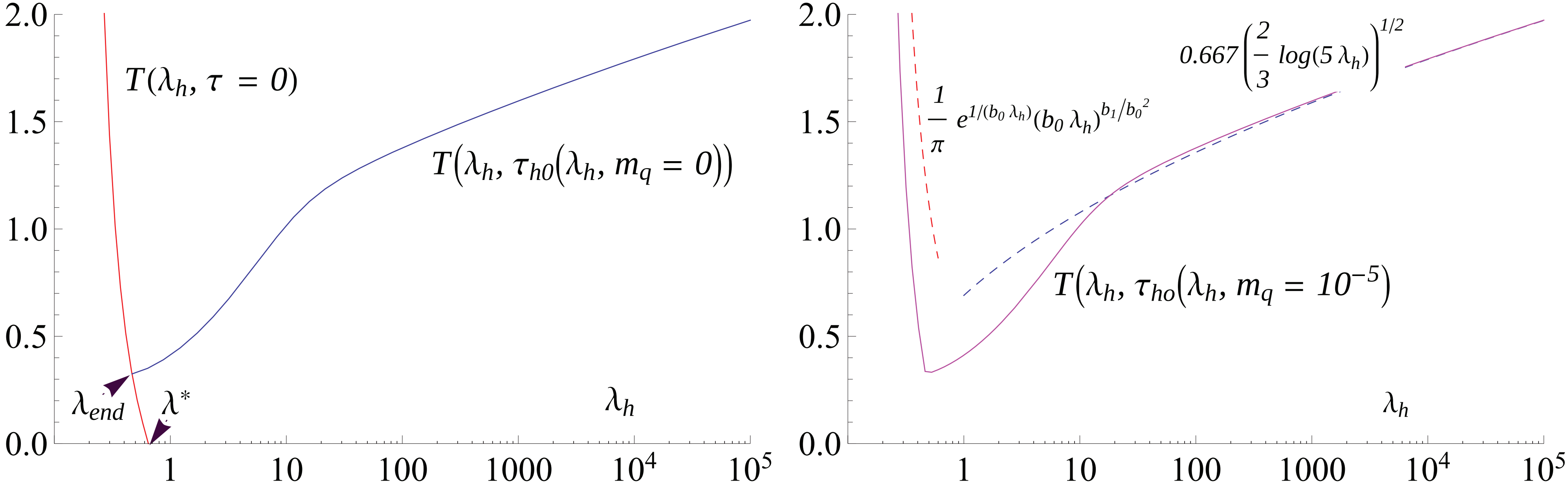

Phase diagram as a function of quark masses

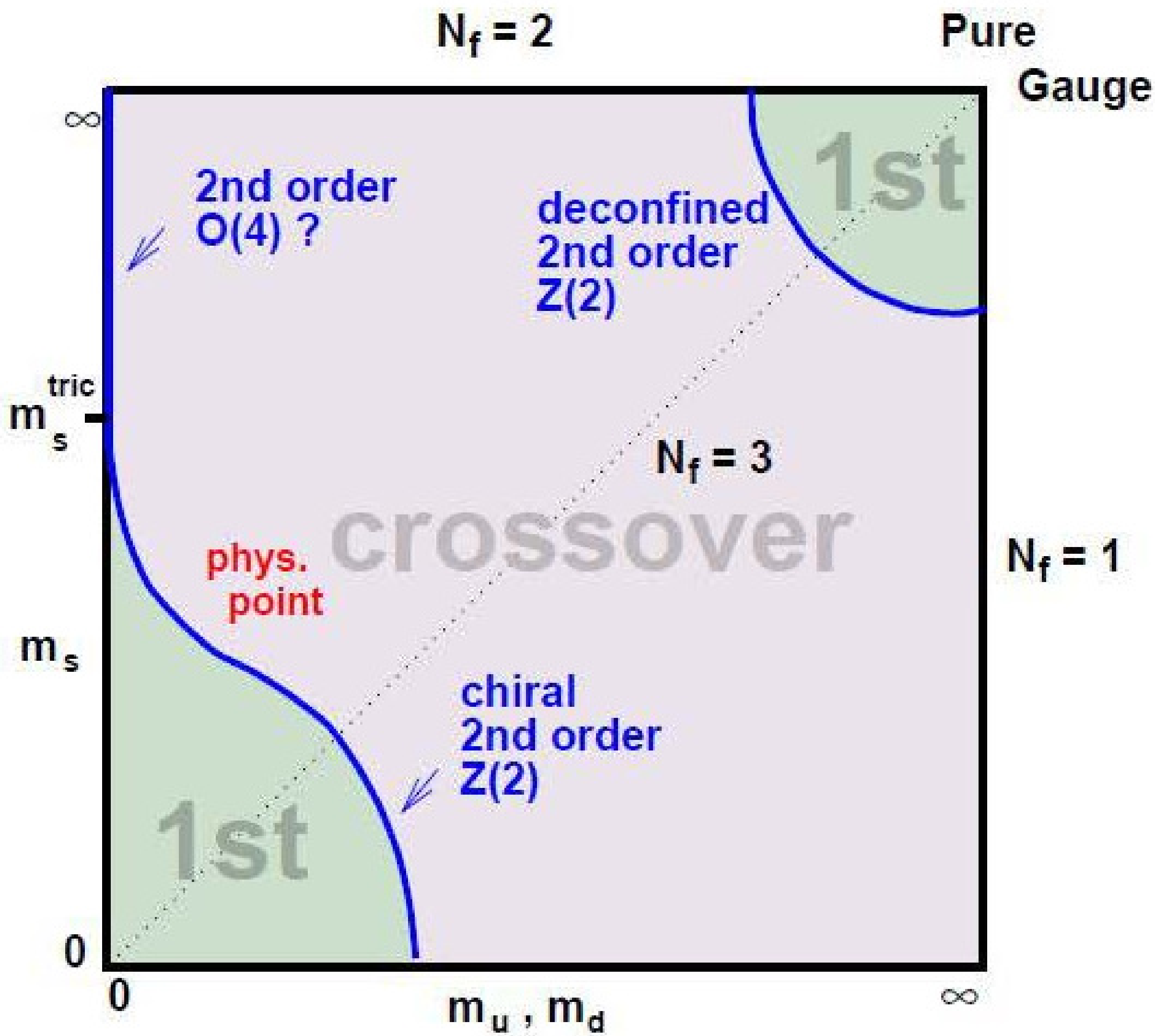

Detailed plan of the presentation

- Title page 0 minutes
- Introduction 5 minutes
- The 't Hooft Large N_c limit 7 minutes
- The Veneziano Limit 8 minutes
- The Veneziano Limit in string theory 11 minutes
- The Banks-Zaks region 14 minutes
- Walking, Technicolor, S-parameter, Dilatons 19 minutes
- Strategy 20 minutes
- The holographic models:glue 23 minutes
- The holographic models:flavor 25 minutes
- Fusion 29 minutes
- Parameters 30 minutes
- Condensate dimension at the IR fixed point 32 minutes